Buckling Restrained Braced Frame with All-Bolted Gusset Connections

PATRICK S. MCMANUS, ADDISON MACMAHON and JAY A. PUCKETT

ABSTRACT

A braced-frame, lateral-load-resisting system was developed in which inelastic deformations due to seismic loading were intended to be isolated to easily replaceable buckling restrained braces (BRB). Bolted brace-to-gusset and gusset-to–beam and column connections were utilized to facilitate simple brace and gusset plate installation and replacement. Full-scale testing using two BRBs was executed to assess performance. Analytical frame models were developed using the nonlinear load-deformation characteristics of the braces. The experimental and analytical results were compared to validate reasonable nonlinear parameters for industry use.

All-bolted brace connections designed per AISC requirements provided adequate capacity to develop the BRBs. With proper detailing, inelastic deformations can be isolated substantially to the BRBs such that a repairable system is achieved. Load-deformation data for individual braces as provided by the supplier can be used to create reasonable analytical models for frames designed with all-bolted connections.

Keywords: buckling restrained braced frames, bolted brace connections, nonlinear analysis, performance-based seismic design.

INTRODUCTION

According to the Hazards U.S. Multi-Hazard (HAZUS) analysis performed by the Federal Emergency Management Agency (FEMA), the costs associated with a catastrophic seismic event are significant (2008). However, it can be argued that the many indirect long-term costs—which are difficult to measure and admittedly neglected by FEMA—may have even greater impact. The long-term societal effects a catastrophic event can have on an area can necessitate years and perhaps decades of recovery. This is evidenced in the United States by the aftermath of Hurricane Katrina and, more recently, the 2011 Virginia earthquake. Several seismic events worldwide in recent years, such as the 2011 Christchurch, New Zealand, earthquake, further illustrate the point. By mitigating the initial impact of a significant seismic event and, more importantly, by reducing the direct costs and duration of repair and recovery for the building inventory in a given area, indirect long-term costs can be dramatically reduced.

Seismic-load-resisting systems for structural steel buildings have undergone considerable evolution over the past two decades. The seismic design criteria adopted by reference in the 2009 International Building Code (IBC) are based upon the performance objective of collapse prevention, assuming a maximum considered earthquake (MCE) with a return period of 2,475 years (2% probability of exceedance in 50 years) (FEMA, 2003). The collapse prevention (S-5) performance objective, as described within ASCE 41-06, "Seismic Rehabilitation of Existing Buildings," allows for considerable inelastic deformations within primary members such that a structure subject to the MCE likely has little residual lateral-load-carrying capacity and cannot be economically repaired (ASCE, 2007). ASCE 41-06 defines higher discrete performance objectives as life safety (S-3) and immediate occupancy (S-1), as well as intermediate objectives damage control range (S-2) and limited safety range (S-4). These higher performance objectives are typically evaluated in consideration of an earthquake of lesser magnitude than the MCE, such as the design basis earthquake (DBE). In the context of ASCE 41-06, the DBE represents an event with return period of 474 years (10% probability of exceedance in 50 years). While some structures designed in accordance with the IBC 2006 or IBC 2009 may inherently achieve higher performance levels for the DBE, ASCE 41-06 indicates that a structure meeting the life safety performance objective may still be beyond economical repair. The resulting expense to the owner or insurer from a seismic event of similar significance could be economically devastating.

As can be seen by various systems described in the 2005 AISC *Seismic Provisions for Structural Steel Buildings* (AISC, 2005a), achieving the design objectives of current building codes in steel-framed buildings is primarily accomplished by proportioning elements such that specific major components experience inelastic deformations. The 2005 *Seismic Provisions* were current at the time of this research

Patrick S. McManus, Structural Technical Director, Martin/Martin, Inc., Lakewood, CO (corresponding). E-mail: pmcmanus@martinmartin.com

Addison MacMahon, Design Engineer, Martin/Martin, Inc., Lakewood, CO. E-mail: amacmahon@martinmartin.com

Jay A. Puckett, Associate Dean and V.O. Smith Professor, Department of Civil & Architectural Engineering, University of Wyoming, Laramie, WY. E-mail: puckett@uwyo.edu

and are referenced in this paper. Components that connect major lateral-load-resisting elements, as well as components that are not intended to resist lateral loads, are anticipated to remain substantially elastic and undergo minimal damage. While the idea of isolating large deformations to anticipated components and locations has considerable merit, the current design methods by which this concept is applied pose some possible inefficiencies, including potentially detracting from the reparability of the structural system.

The controlled and predictable yield of major components has resulted in considerable limitations on global and local member geometry. To achieve desired compactness requirements and slenderness ratios, often beam, brace and column sections gravitate to sectional areas well in excess of those required to resist loads derived from the load combinations of the applicable building code. This places considerable force demands on connections, which in seismic applications are typically required to develop the expected yield strength of the primary member. The results are increased material and connection costs.

To develop the expected yield strength of members such as beams or braces, welded connections are typically required. The reason is the area reduction due to holes for bolted connections typically results in inadequate available tensile strength at the net section to develop the required expected yield strength of the member. Usually, some magnitude of welding must occur in the field, which is arguably the most expensive process in steel construction. This may increase the relative cost of the steel frame, making it less competitive with other lateral-load-resisting systems.

Primary structural components such as beams and columns are extremely expensive by structural standards and difficult to adequately repair or replace, particularly when equipped with fully welded connections. Typically, these components, by design, are fully integrated with the overall structural scheme and, in most cases, are relied upon to carry gravity loads in addition to lateral loads. Therefore, as noted previously in relation to ASCE 41-06, replacement of such components once significantly damaged is often unrealistic, leaving complete demolition and replacement of the building as the only viable option. New innovations in seismic-load-resisting systems have recognized that the approach of isolating inelastic deformations to primary, permanently attached components may be flawed when reparability is a primary objective. By instead isolating inelastic deformations to easily accessible, bolted components that can be relatively inexpensively removed and replaced, a repairable seismic-load-resisting system can be achieved.

Herein, a *repairable system* is defined as a frame where inelastic deformation has been accommodated in such a way that the damaged element can be reasonably removed from the frame after a seismic event and replaced with a similar element, e.g., a buckling restrained brace (BRB). Connections and/or other members are designed to remain substantially elastic and can therefore be reused.

Repairable seismic-load-resisting systems pose several advantages. Components that are relatively easily replaced characteristically exhibit easy initial installation. Therefore, the field labor associated with initial installation of a repairable system may be reduced over the current labor-intensive installation processes described previously. Reduction in field labor typically translates to reduction in overall cost and schedule. Additionally, structures with enhanced potential to be viably salvageable after a significant seismic event are likely marketable to owners and insurers. It is recognized that a repairable structure does not reduce the deformations and associated damage of nonstructural components nor does it address the repair of those components. Enhanced detailing of nonstructural components may be required to ensure a building with a repairable structural system is salvageable.

To adequately address a wide spectrum of building program needs, proposed repairable connections and components have been developed for moment frame (McManus and Puckett, 2011) and braced frame systems. Only the braced frame system—referred to as fully bolted, buckling restrained braced frames (BRBF)—is addressed herein. Two full-scale BRBF one-bay, one-story frames were tested. The brace-to-gusset, gusset-to-member and member-to-member frame connections were fully bolted. The BRB could be replaced by unbolting the damaged brace and replacing it with a new one. In the present test series, a Star Seismic BRB (WC250, implying a core yield strength of 250 kips) was initially installed in the test frame. The translation/drift regimen of Appendix T of the 2005 AISC *Seismic Provisions* was used based on a maximum drift of 2%. The BRB and connections performed well, and the system illustrated robust and stable hysteric behavior.

The frame was re-plumbed and another brace (WC200) was installed. Testing of the second brace again employed the regimen prescribed in the AISC *Seismic Provisions* with a 2% maximum drift. The frame was examined for damage and then tested again under the AISC regimen adjusted for 3% maximum drift. The brace and the connections performed well. The hysteric behavior again was stable for all cycles. Because 3% was the limit of the test configuration, the test series was ended.

The test regimen of Appendix T of the 2005 AISC *Seismic Provisions* is intended to achieve a maximum story drift equal to twice the design story drift. The proportioning of structural elements to achieve the design story drift can vary considerably as the result of many factors, such as analysis methodology and building classification within the applicable building code. Consequently, it is beyond the scope of this paper to identify a specific magnitude of earthquake for which a structural system utilizing the BRBF connections

described herein is economically repairable. Rather, the intent is to demonstrate adequate performance in accordance with requirements of the AISC *Seismic Provisions* and enhanced reparability compared with other structural systems or BRBF systems with welded gusset-to-beam/column connections.

This article contains the test description and results for global behavior for the frame and local strains in areas of interest. The information from these tests was used to develop recommendations for proportioning and configuring the members and connections. In summary, the concept of designing a structural frame with enhanced reparability appears to be viable. Connection details can accommodate the significant drift requirements. The replacement of the brace was demonstrated.

BACKGROUND

Buckling Restrained Braced Frames—Overview

In high-seismic regions, it is probable that structures designed in accordance with IBC 2009 will experience inelastic deformations from a seismic event during the course of its service life (McManus and Puckett, 2011). The inelastic deformations can occur in several ways, depending on the goals and type of system being designed. The BRBF system uses diagonal-brace elements, which are designed to yield in a predictable and favorable manner. Figure 1 illustrates a typical BRBF and the BRB application in the two-story X-bracing configuration. These gusset plates are welded to the columns and beams.

Figure 2 illustrates a schematic of a BRB made of three distinct sections: the core that is design to yield, the transition zone and the extension plate. The steel core and transition are encased in a grouted tube that restrains the core from buckling under compressive loads. Typical cross-section details are illustrated in Figure 3. The details for the tested BRBs are changed to accommodate bolting. The BRB details are provided in McManus, Puckett and MacMahon (2011).

Repairable BRBF Seismic Systems

Because the core of the brace need only be proportioned to provide sufficient stiffness to meet story drift requirements

Fig. 1. BRBF Example: Lawrence Berkeley National Lab (Star Seismic).

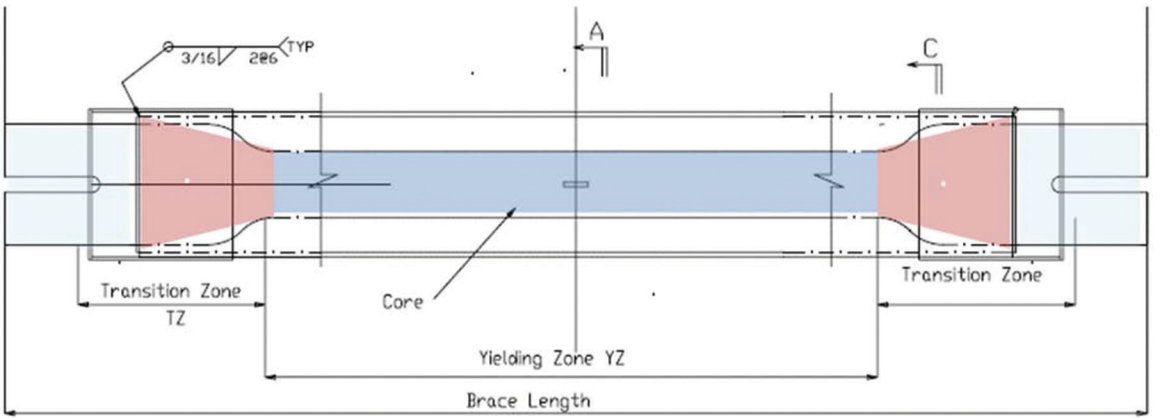

Fig. 2. Schematic of a BRB.

or to carry the loads from the applicable building code without consideration of buckling, the required strength of the connections to develop the expected yield of these braces is typically less than that of other types of seismic braced frames. Forces to the connections can therefore be adequately addressed with bolted connections. However, tests of BRBF assemblies to date have consisted primarily of welded connections between the gusset and column and almost entirely of welded connections between the gusset and beam [refer to Lopez et al. (2004) and Thornton and Muir (2009) for examples with associated references]. Test results in braced frame systems often result in significant damage at the interface between the gusset and beam or column due to the large rotations induced at the connection under the large story drifts simulated in seismic testing (Thornton and Muir, 2009). Therefore, even if the BRBF were bolted to the gusset but welded to the primary members, a repairable system would not be achieved should damage to the gusset occur during a seismic event. By bolting the gusset to the brace as well as the beam and column as shown in Figure 4, a repairable system can be produced.

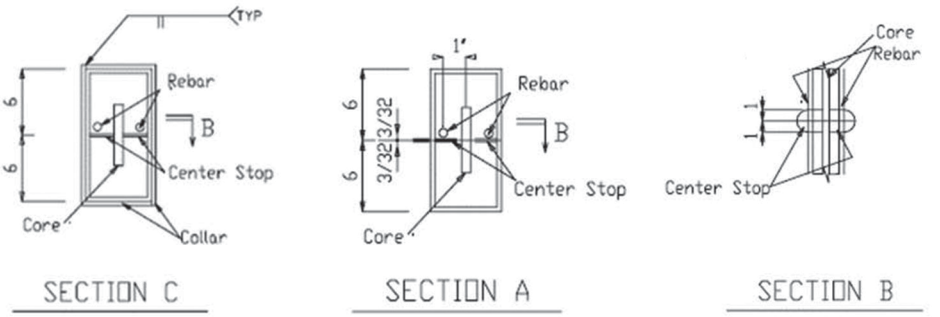

Fig. 3. Typical BRB section details.

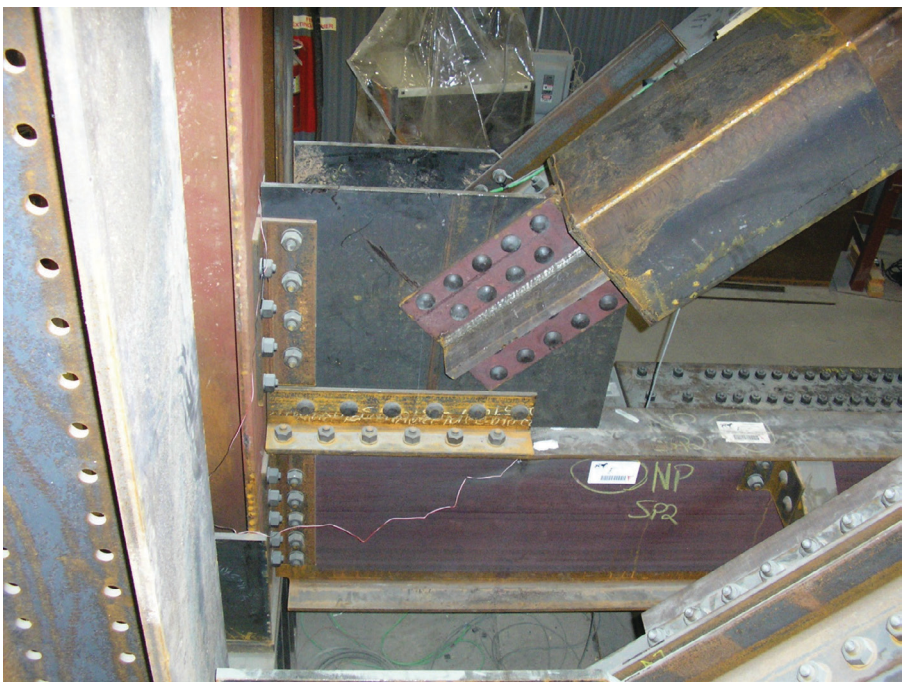

Fig. 4. Fully bolted buckling restrained brace connection prior to test.

RESEARCH OBJECTIVES

The primary goal of this research was to evaluate fully bolted BRBFs as repairable seismic-load-resisting systems through experimental testing. A second goal was to verify that fully bolted connections designed using then-current AISC provisions adequately developed the BRB at code-required story drifts. Finally, the third goal was the development of linear and nonlinear analysis procedures that adequately represent the behavior. Recommendations for design as well as linear and nonlinear modeling were developed.

BRACE AND FRAME DESIGN

Beam and Column Design

Primary framing members for the test frame and reaction frame were intended to remain elastic during the tests. Initial design was consistent with simple hand methods that are common in professional practice. The adjusted brace strength of the WC250 in compression was assumed to develop in the brace. The adjusted brace strength in compression is defined within the 2005 AISC *Seismic Provisions* as $\beta\omega R_y P_{ysc}$, where β is the compression strength factor, ω is the strain hardening factor, R_y is the ratio of expected yield stress to minimum specified yield stress, and P_{ysc} is the axial yield strength of the core (AISC, 2005a). The ratio of compression strength to tension strength, β, was assumed to be 1.14 based on test data from the University of Utah (Romero et al., 2007). From the same data, the hardening factor, ω, was assumed to be 1.58. The β and ω factors were calculated based on the anticipated strains in the steel core at twice the design story drift in accordance with the 2005 AISC *Seismic Provisions*. Because Star Seismic performed tensile coupon tests on the braces provided for the testing herein, R_y was taken as 1.0. The forces in the primary framing members associated with the assumed adjusted brace strength were calculated using statics, and the strength was checked using standard AISC LRFD procedures. Members were assumed to have pinned ends with an effective length factor, K, of 1.0. All wide-flange sections were ASTM A992 steel. Coupon tests of connection, beam and column material were not performed.

Seismic compactness criteria and available sections from the fabricator assisting with the project were also considered in the design. The lightest seismically compact nominal 14 in. by 14 in. (356 mm by 356 mm) wide-flange shapes (W14×132) were used for the columns in the test frame (see Figure 5). The high and low ends of the BRB (diagonal orientation) were initially configured such that the actuator force would be delivered to the brace through the upper beam of the test frame. Consequently, the upper beam (W21×62) was initially sized to carry this force. It was also sized based on availability from Puma Steel, flange geometry to adequately receive bolted connections, and flange and web compactness ratios within the maximums allowed by the 2005 AISC *Seismic Provisions*. However, the brace direction was switched later in design such that the actuator and brace would be in compression at the same time. This was done to ensure that the strength of the brace was developed recognizing the strength of the brace and capacity of the actuator were both greater in compression than in tension. With the new configuration, the upper beam of the test frame theoretically became a zero force member.

The lower beam of the test frame (W24×55) transferred the horizontal component of the brace force through a

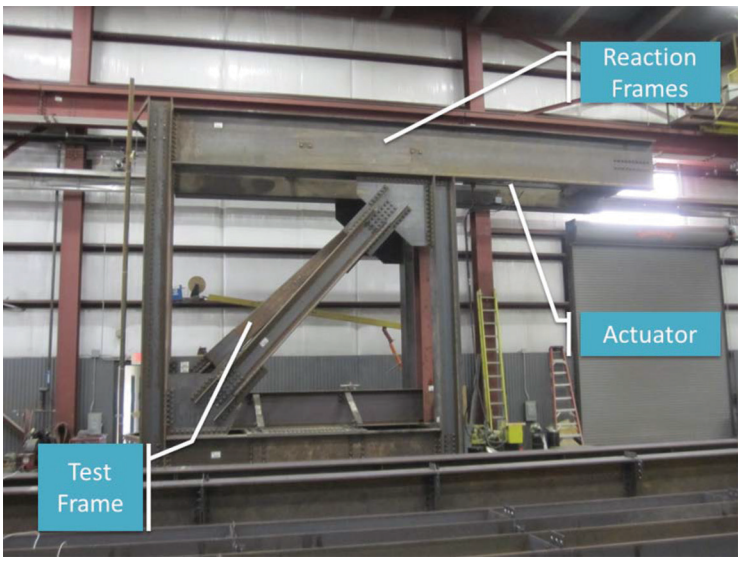

Fig. 5. North view of frame.

diaphragm plate to the reaction frame. This beam was designed assuming strong-axis brace points at the member ends and weak-axis brace points at the ends and at third points. Strong-axis eccentricity was not considered in the initial design because eccentric forces were assumed to be easily resolved through the frequent bottom-flange connections to cross beams within the reaction frame. The lower beam was sized using similar considerations to the upper beam, except that the web compactness ratio was slightly above the AISC maximum seismic compactness limit. Exceeding the web seismic compactness ratio was intentional to challenge the beam capacity and ensure, through successful performance, that all compact sections could be assumed to perform adequately. Additionally, the web of the lower beam was slender for shear strength calculations per the 2005 AISC *Specification for Structural Steel Buildings* (AISC, 2005b).

Primary members within in the reaction frame were also chosen based on material availability but were primarily intended to provide elastic stiffness several times that of the test frame. Consequently, demand-to-capacity ratios in the members were relatively small, and seismic compactness was not considered. Adequate capacity of all members was verified in later analytical modeling.

Design of BRB-to-Frame Connections

In general, for any bolted joint in the seismic-load-resisting system (SLRS), the joint can be designed as a bearing-type connection if standard holes are used in all plies, but it must be constructed as slip-critical. Thus, the bolts must be pretensioned, and the faying surface must meet at least class A requirements (class B and C faying surface requirements would also be acceptable). This requirement is intended to limit deformations within the joint during an earthquake. An exception to this requirement is for bolted joints at diagonal brace connections. In this case, oversized holes are permitted in one ply of connected interfaces provided the connection is designed as slip-critical. This exception was added to the 2005 AISC *Seismic Provisions* based on feedback from erectors, who indicated that fit-up of bolted brace connections was very difficult with standard holes.

Finally, for any bolted joint in the SLRS, the nominal bearing strength cannot be taken greater than $2.4dtF_u$, where d is bolt diameter and t and F_u are the thickness and rupture strength of the material being connected, respectively. Chapter J of the AISC *Specification* permits the nominal bearing strength to be taken as high as $3.0dtF_u$. However, at this level, significant hole elongation occurs. Consequently, in order to again limit movement at bolted joints during an earthquake, the AISC *Seismic Provisions* limit the nominal bearing strength.

The uniform force method was used to determine the force distribution in the brace connections. The uniform force method determines force distribution to connection components and primary members based on the geometric extents of the primary members being connected. Further description of this method can be found in the 13th edition of the AISC *Steel Construction Manual* (AISC, 2005c). Special case 2, as defined by AISC, was used at the upper brace connection to theoretically eliminate shear to the beam. This addresses multiple force distribution approaches through the testing. The gusset plate at the upper connection was attached to the column web, whereas the gusset was connected to the column flange at the lower connection to incorporate multiple framing conditions into the testing as well. Figures 6 and 7 depict the connections at the lower and upper end of the brace, respectively.

All plate and angle material was ASTM A36. All bolts were ⅞-in. (22-mm) diameter. ASTM A325 bearing bolts with threads excluded from the faying surfaces were used to connect angles to gusset plates and primary members. ASTM A490 bolts were used to connect the BRB to the gusset plates using slip-critical connections. A class A faying surface preparation was provided with standard holes in the gusset plates and oversized holes in the connection plates on the BRB.

The probable brace forces used for connection design were developed in accordance with the 2005 AISC *Seismic Provisions* using β and ω factors recommended from tests of Star Seismic braces at the University of Utah (Romero et al., 2007), discussed previously regarding member design. Star Seismic uses these factors in practice, and the intent was to be consistent with its typical design approach. Standard Load and Resistance Design (LRFD) ϕ factors were applied in designing for each of the connection limit states.

Governing design limit states of the gusset-to-beam/column connections were bolt shear, prying action and bolt bearing on the gusset. Slip-critical joints with ASTM A490 bolts in oversized holes were used to connect the braces to the gussets. Thus, slip-critical shear values governed the brace-to-gusset connections. Demand/capacity ratios varied between roughly 0.9 and 1.1 for these governing limit states. The 10% overstresses were typically on prying action checks in the connection angles. The overstress was intentional to challenge the design, recognizing weak-axis bending of the angles often governs strength and stiffness in all bolted connections.

EXPERIMENTAL TEST SETUP

Test Procedure, Arrangement and Equipment

Full-scale testing of the braces first involved one trial run on the test specimen without any brace installed. The intent of the trial run was to verify that the data acquisition software would work properly with the instrumentation. Testing of the two buckling restrained braces was performed per the provisions of Appendix T of the 2005 AISC *Seismic*

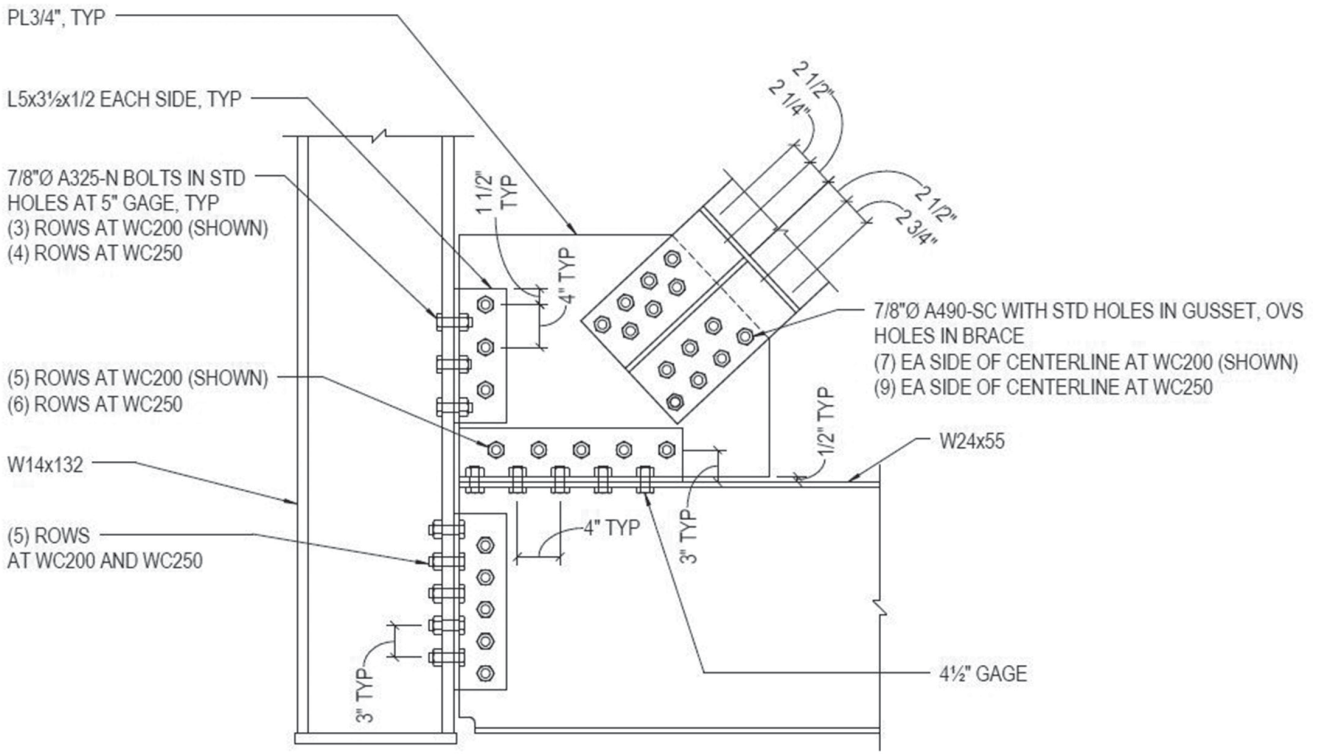

Fig. 6. Brace connection detail at lower brace end.

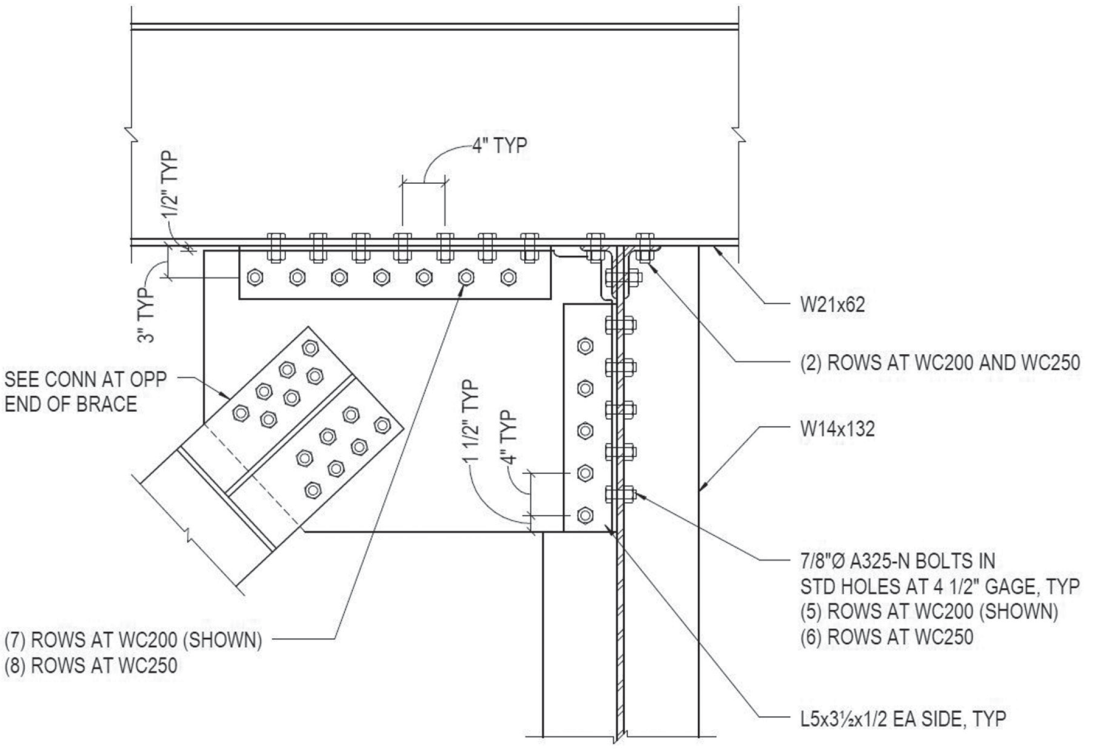

Fig. 7. Brace connection detail at upper brace end.

Provisions. The initial test regimen was based on a maximum of 2% drift in the test frame and the required cumulative inelastic deformation of 200 times the yield deformation of the brace. To account for deformations external to the steel core, such as in connection components and primary members, the yield deformation used for development of the test regimen was conservatively calculated assuming a work point–to–work point steel-core length of 246 in. (6250 mm). Coupled with an assumed yield stress of 43 ksi (296 MPa), the yield deformation was approximated as 0.365 in. (9.27 mm). The actual yield deformations calculated using the average yield stress for each steel core from coupon tests and the steel-core length from shop drawing details were 0.160 in. (4.06 mm) and 0.166 in. (4.21 mm) for the WC250 and WC200, respectively. Using the larger of these values, the actual cumulative inelastic deformation requirement for the braces was 33.2 in. (843 mm). Upon successful completion of the test on the WC200 brace, the regimen was reconfigured based on a maximum drift of 3% and successively applied to the same WC200 brace and brace connections. The same beams, columns and beam-to-column connections were used for both tests.

A reaction frame with an actuator rated to produce 600 kips (2850 kN) of push force and 450 kips (2140 kN) of pull force was constructed to perform testing as diagrammed in Figure 8. The reaction frame was arranged so that lateral bracing of the test frame had minimal restraint in the plane of the test. The orientation of the actuator was such that the pushing force would put the BRB into compression and the pulling would create tension in the brace. The actuator was used to produce translation-controlled loading of the test frame. The accumulated translation of the test frame was calculated from the collection of top translation relative to base translation at the outer test frame column.

The test specimen was instrumented with two string potentiometers; one linear potentiometer; pressure gauges on the actuator to determine load to the test frame; and multiple strain gauges on beams, connection angles and the gusset plate (see Figure 8).

A string potentiometer was mounted at the top of the test specimen on the outer column to measure the total drift (see designation A in Figure 8). A linear potentiometer was mounted on the outer column to measure any movement at the bottom (see designation B in Figure 8). A second string

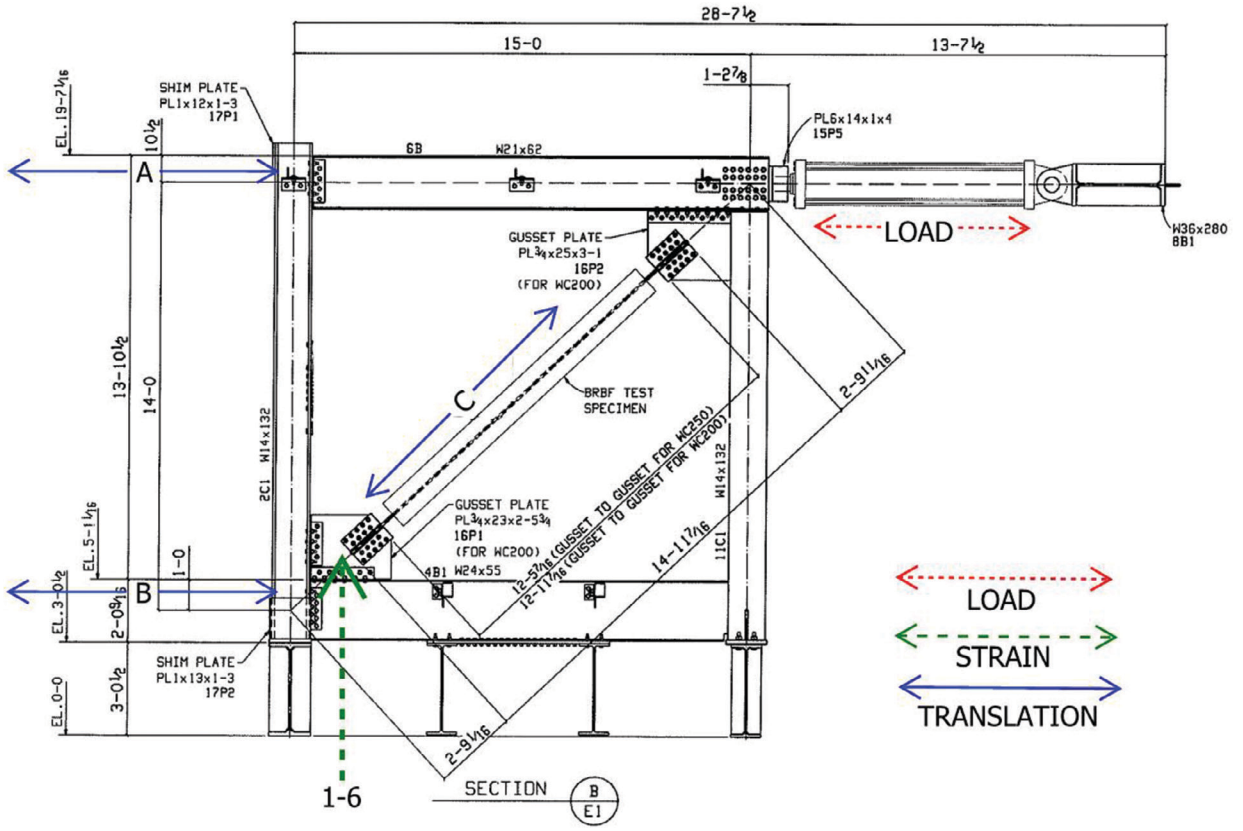

Fig. 8. BRBF test frame instrumentation.

potentiometer was mounted along the BRB long axis with mounting points near the ends of the reduced yield zone section to measure total axial deformation of the steel core (see designation C in Figure 8).

The strain gauge orientation for the first test on the WC250 was primarily located around the bottom gusset plate connecting the brace to the beam and column. Strain gauge 1 (SG1) was mounted vertically on the gusset plate. SG2 was mounted on the gusset plate aligned with the brace. SG3 was mounted horizontally near the same location as SG1 and SG2 with the intent of capturing the in-plane state of stress in the gusset (see Figure 9).

SG4 was located on the angle connecting the gusset plate to the bottom beam and was placed near the outermost bolt hole. SG5 was placed under the top flange of the bottom beam directly below SG4 (see Figure 10). SG6 was placed on the outstanding leg of the angle connecting the gusset plate to the column next to the outermost bolt hole, similar to SG4 (see Figure 11).

For the WC200 test, SG1 through SG5 were in the same locations as in the WC250 test. However, SG6 was placed on the web of the bottom beam, see Figure 12.

The initial trial run of the data acquisition software, with gusset plates in place but no brace, provided information to adjust the software, but also unintentionally resulted in pulling the test frame to a drift of nearly 3%, which caused local web yielding and web crippling in the bottom beam in the test frame. Note the beam was intentionally slightly outside the limits for seismic web compactness, and the web was slender for shear. The proportions were selected to suggest any compact section would perform adequately under similar loading. However, the mishap now leaves a question as to whether web yielding and crippling would have occurred if a compact section had been used. The excessive deformation was the result of an error in the software that pushed the frame past the target deformation and continued until the program was shut down manually. Also, it was determined that the original automated software could not function properly due to high load spikes produced when joints at the gusset plate–to–beam and column connections that were designed with bearing bolts—but constructed as slip-critical in accordance with the AISC *Seismic Provisions*—slipped into and out of bearing. The pressure gauges in the actuator were not designed for dynamic loading and thus would read pressures beyond the recordable limits of the sensors when small, sudden movements in the frame occurred. Based on these limitations, it was decided to conduct the test manually, with one computer operator controlling the actuator until the desired test frame displacement was reached. This approach proved to be adequate and was used for all subsequent tests.

The data acquisition software used to collect translation, pressure and strain data was National Instruments' LabView 2010, version 10.0.0. All strain gauges used were Vishay Micro-Measurements and SR-4 general-purpose strain gauges. The digital string pot used on the braces was

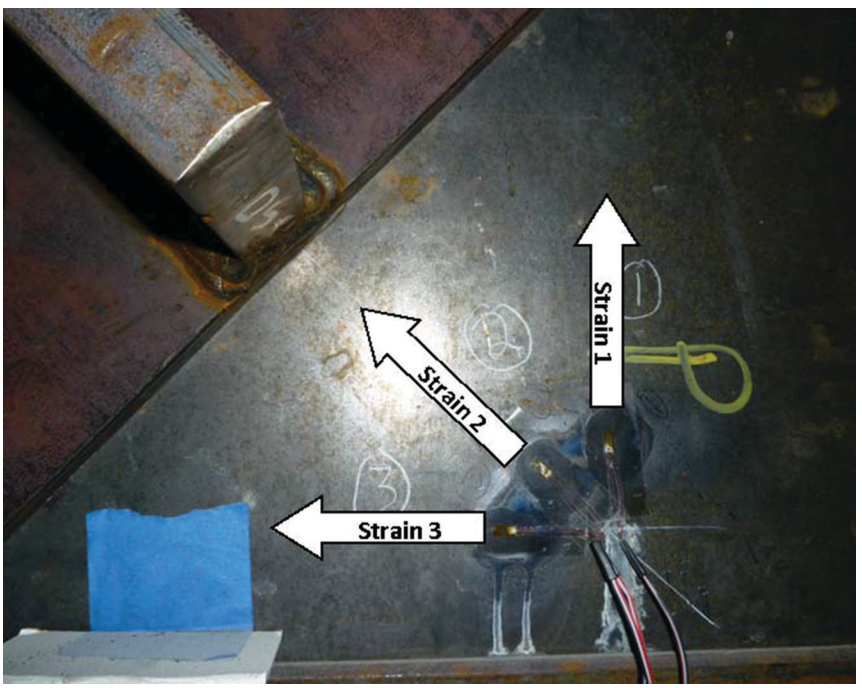

Fig. 9. WC250 strain gauges.

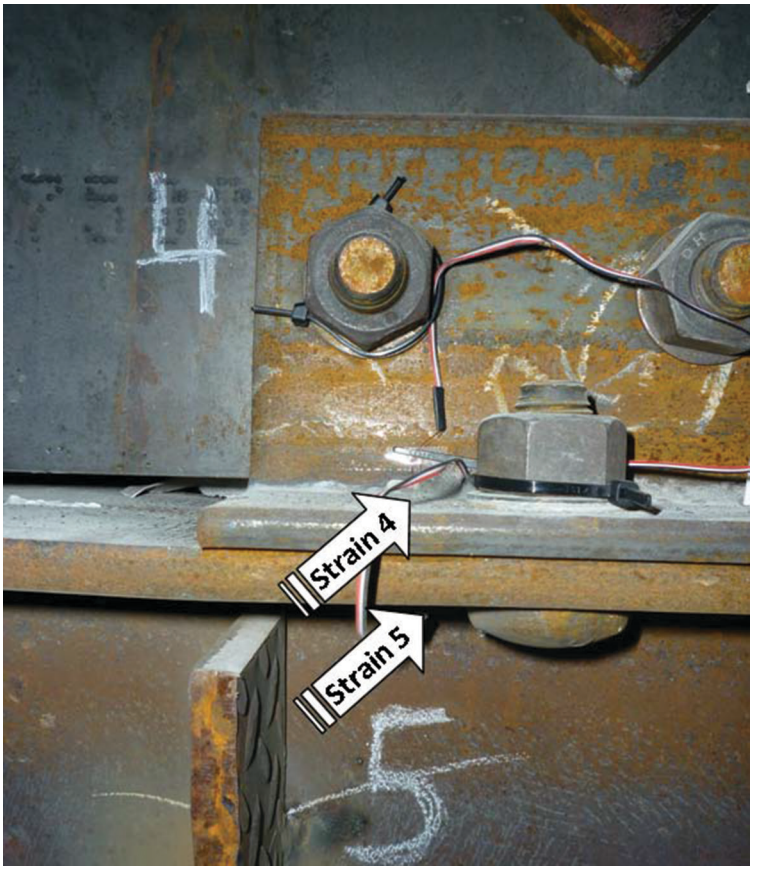

Fig. 10. WC250 strain gauges.

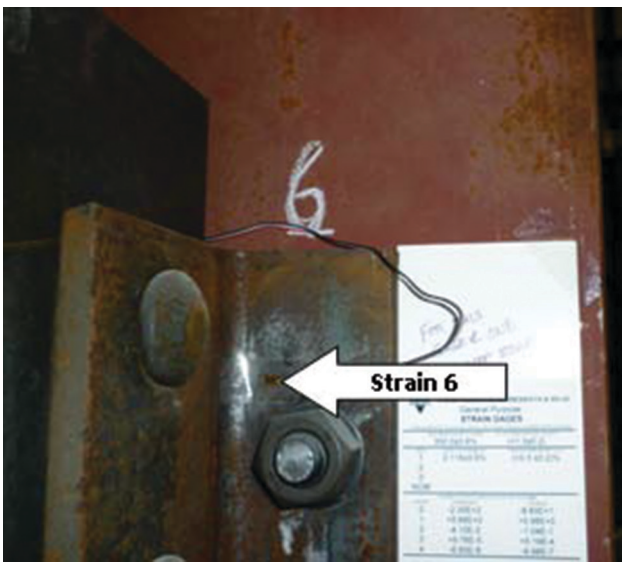

Fig. 11. WC250 strain gauges.

Celesco model SR1E, with an incremental encoder output signal and a stroke range of 125 in. (3180 mm.) The smaller string pot mounted at the top of the column with a 10-in. (254-mm) stroke was UniMeasure model JX-EP-10. The linear potentiometer used at the base of the outer column was ETI Systems model LCP12S-100. Details are provided in the associated manuals (see McManus et al., 2011).

EXPERIMENTAL RESULTS

Test 1 Results: WC250 Brace

Due to "banging" from built-up load and subsequent slip in the joints, much of the information was simply filtered to remove transients. Only data corresponding to the system in motion were filtered. There was negligible translation at the base of the test specimen, as expected. The applied load versus displacement history exhibited stable and repetitive behavior with positive incremental stiffness (see Figure 13).

Visual inspection of the connection material after the test suggested slip only occurred at connections between the gusset plate and connection angles that attached the beams and columns, which were designed as bearing connections with standard holes. The gusset plate at the connection of the brace, as well as the connection plates on the brace, did not show any of the scarring due to slip noticed at the bearing connections, nor any signs of hole elongation. Consequently, the brace-to-gusset connections that were designed slip-critical appeared to resist the load without slip, as intended.

The test regimen was designed such that the frame cumulative translation would reach 131.6 in. (3343 mm). Actual accumulated frame translation was measured to be 134.5 in. (3416 mm). Because steel-core elongation was not properly measured during this test, the ratio of inelastic deformation to frame translation from the WC200 test was used to approximate the cumulative inelastic deformation for the WC250 test. This is reasonable because steel-core length and yield stress are similar between the two braces. Using the ratio from the WC200 test, the cumulative inelastic deformation for the WC250 was approximately 64.7 in. (1642 mm), which is nearly 400 times the calculated yield deformation and approximately twice the AISC minimum requirement of 33.2 in. (843 mm).

Strain data are shown in Figures 14 through 20. SG1 measures strain on the gusset in the vertical direction. The strain shows an asymmetrical response to load. At an assumed steel modulus of 29,000 ksi (200,000 MPa), the max stress in the vertical direction was 7.2 ksi (50 MPa) at a strain of $\varepsilon = 247\ \mu$. Hereafter, similar data are paired [e.g., (247 μ, 7.2 ksi)], and the results are discussed in terms of stress.

SG2 is consistent with the axial forces from the brace into the gusset plate and matches the hysteresis of the system (symmetric with loading). The max strain and stress are (1300 μ, 39 ksi) at SG2. SG3 measures the strain in

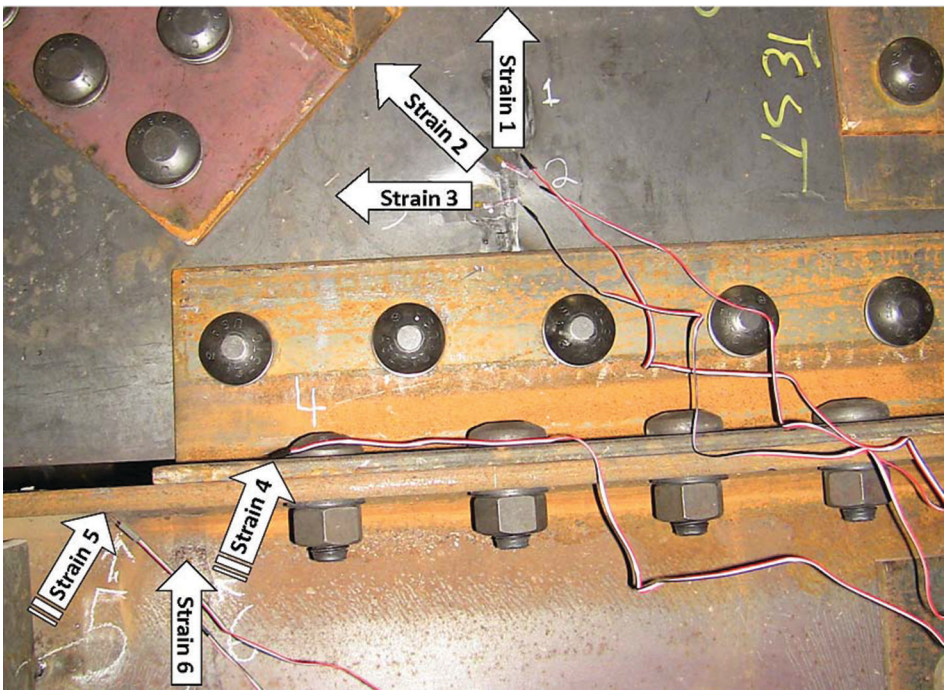

Fig. 12. WC200 strain gauges.

the horizontal direction on the gusset plate along the beam connection. SG3 exhibited behavior similar to SG1 with an asymmetric response to loading, (231 μ, 6.7 ksi). This asymmetric response is to be expected because the load transferred from the brace to the gusset is 43° from horizontal in relation to SG1 and SG3. With this orientation of the brace, the vertical component of strain (SG1) is affected more by tension forces from the brace and less by compression when the gusset is bearing on the bottom beam. The horizontal strain (SG3) is more affected by compression forces from the braces.

SG4 was located along the bottom angle connecting the gusset plate to the bottom beam, positioned perpendicular to the longitudinal beam axis. The gauge was positioned next to a bolt and reported a maximum value of 2100 μ when the brace was in tension and the angles resist forces through bending. This value was largely in excess of the strain corresponding to minimum specified yield stress of 36 ksi

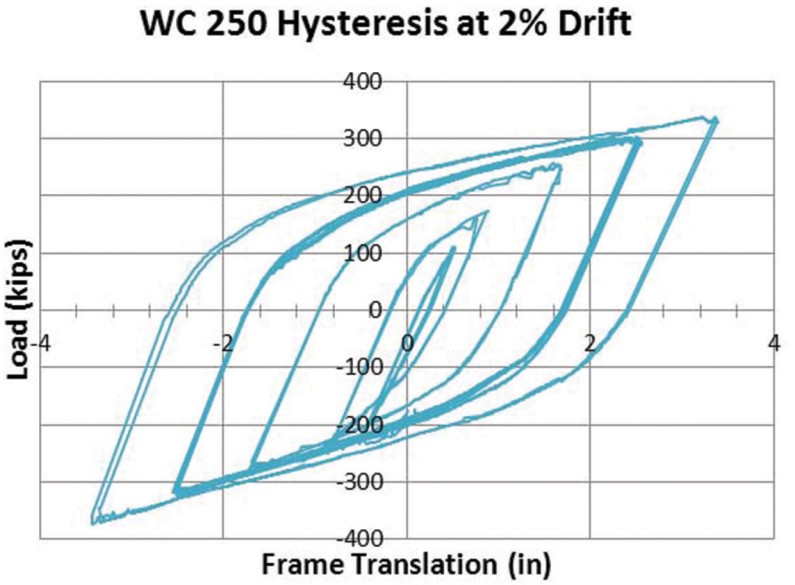

Fig. 13. Test 1 WC250 hysteresis.

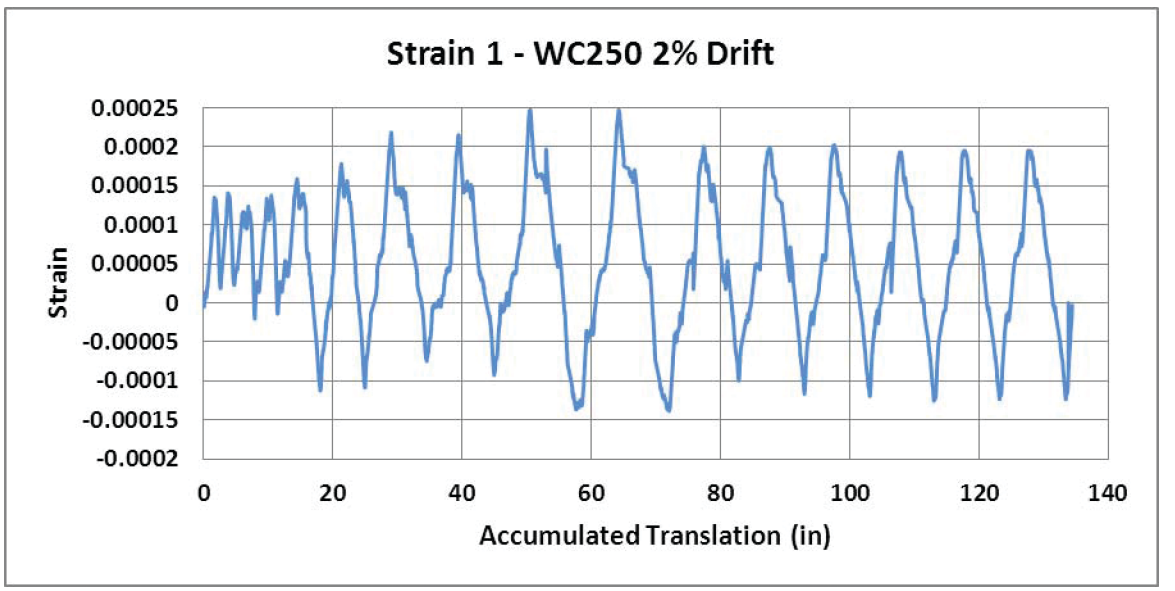

Fig. 14. Test 1, WC250 SG1.

(1200 μ). Much lower values were present when the brace was in compression and the angles were bearing on the beam flange. At the maximum strain recorded in compression, the approximate stress was calculated to be (718 μ, 20.8 ksi). Stress in excess of theoretical yield, or even actual yield if it were known, is not surprising at this location because the stresses vary considerably across the outstanding leg of the angle, and concentrations are likely present near bolts.

SG5 measured strain perpendicular to the length of the bottom beam on the underside of the beam's top flange. The stress does spike close to yield during the two largest displacement cycles at approximately 1840 μ, which is reasonable given the higher rotations of the frame at this point and thus more tension near the bolt holes in the top flange. Similar to SG4, concentrations likely are present near the bolts.

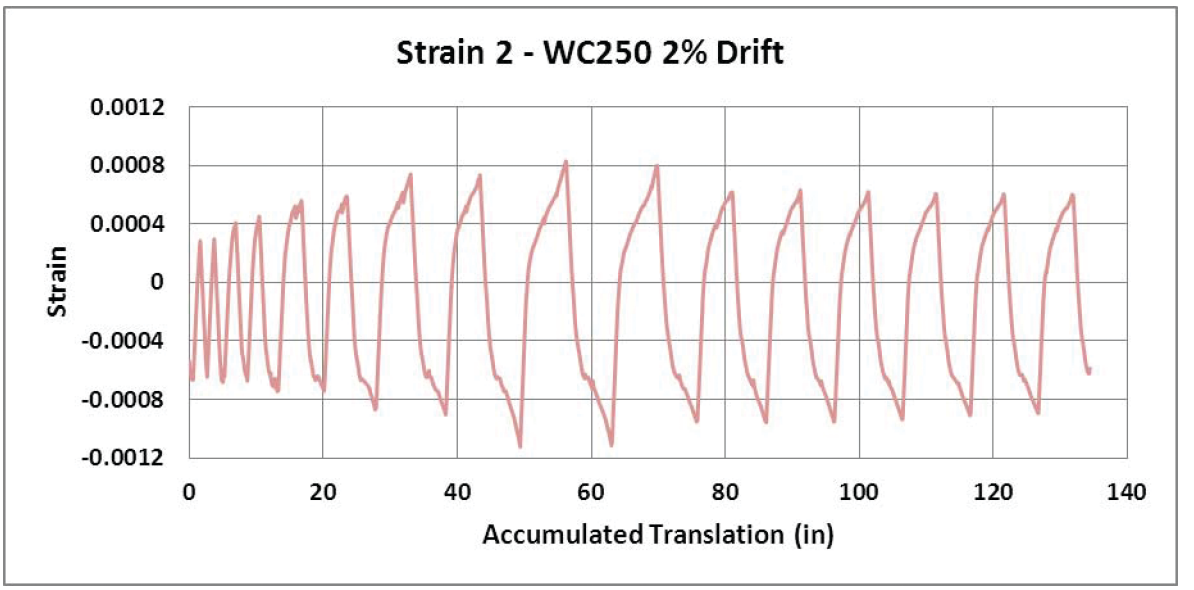

Fig. 15. Test 1, WC250 SG2.

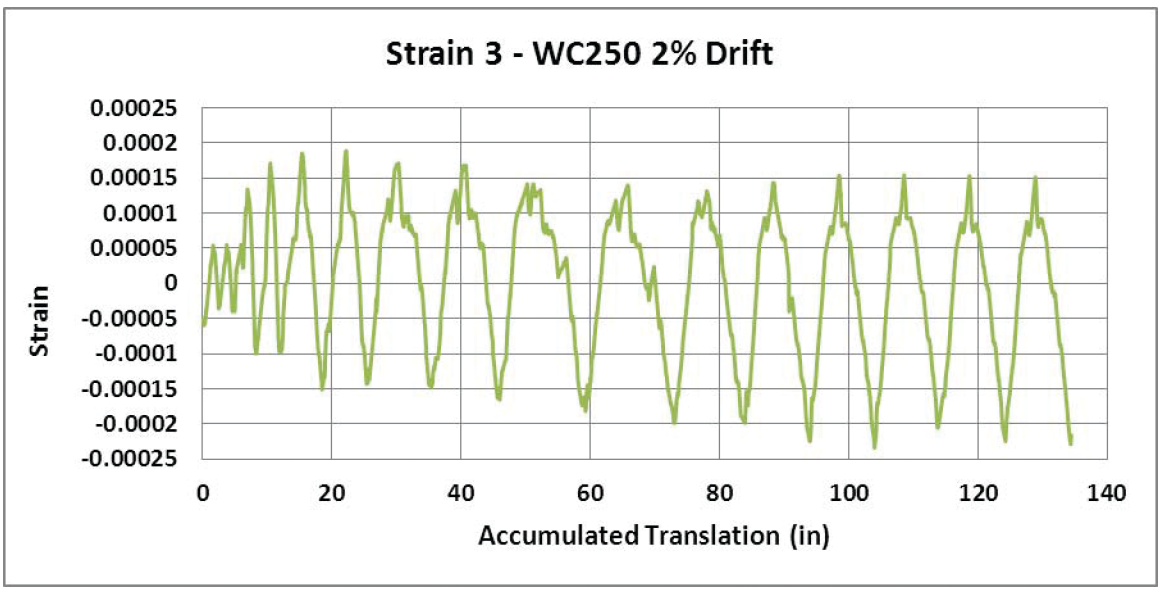

Fig. 16. Test 1, WC250 SG3.

SG6 measures strain in the angle connecting the gusset plate to the column near the outermost bolt in the horizontal direction. This connection shows similar behavior to SG4, with higher strain when the brace is in tension and lower strain in compression (bearing on the flange). The approximate stress measured was (1220 μ, 35.4 ksi), which indicates lower stress in this element than in the angles connected to the beam or in the beam flange.

SG7 was only recorded in the WC250 test and was measured roughly at the work point of the upper beam where the actuator load was applied to the test specimen. Stresses at this point were low, reaching a maximum of near (76 μ, 2.2 ksi). This value suggests approximately 40 kip (178 kN), or 12% of the load in the actuator, was transferred to the beam. Thus, 88% was resisted by the brace. The 40-kip load calculated from the strain data was relatively consistent with

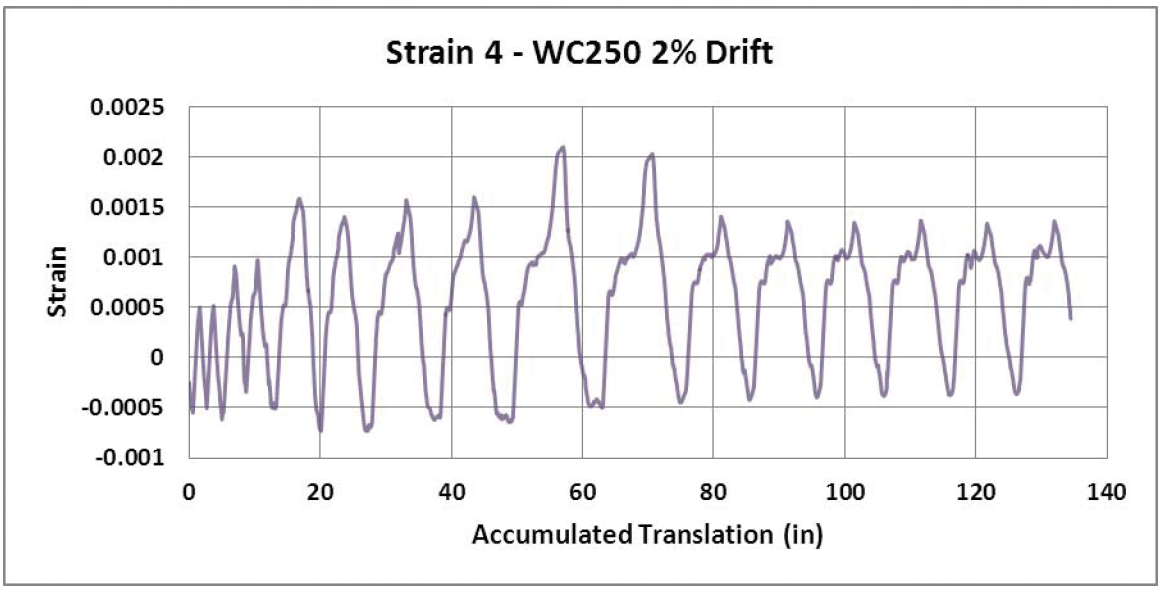

Fig. 17. Test 1, WC250 SG4.

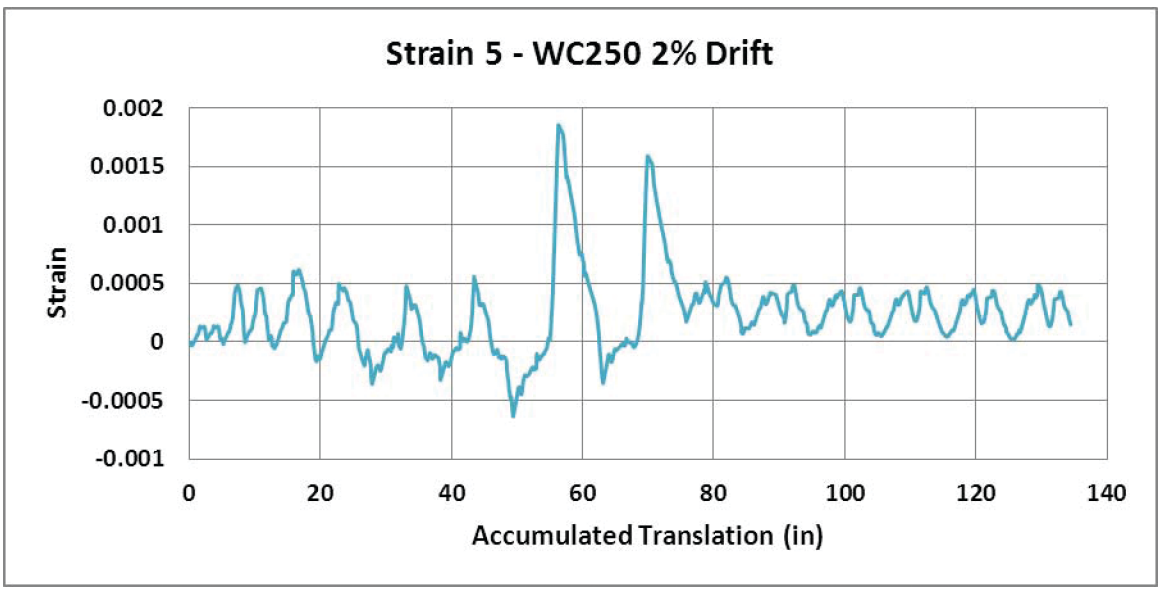

Fig. 18. Test 1, WC250 SG5.

the maximum force recorded during the calibration test with gusset plates installed, but no brace present, under similar translation.

The University of Utah (Romero et al., 2007) reported a maximum force in the WC250 during testing to be 404 kips (1797 kN) in tension and 474 kips (2108 kN) in compression. This project used a connection design axial force in the brace of 435 kips (1935 kN) in tension and 496 kips (2006 kN) in compression. During testing of the WC250, the maximum axial force achieved in the brace was 404 kips (1797 kN) in tension (equal to the University of Utah max under similar strain) and 451 kips (2006 kN) in compression (95% of University of Utah max under similar strain). Brace force was calculated geometrically based on the force in the actuator and adjusted for the aforementioned assumption that 88% of the actuator force was resisted by the brace due to the 12% contribution of frame action.

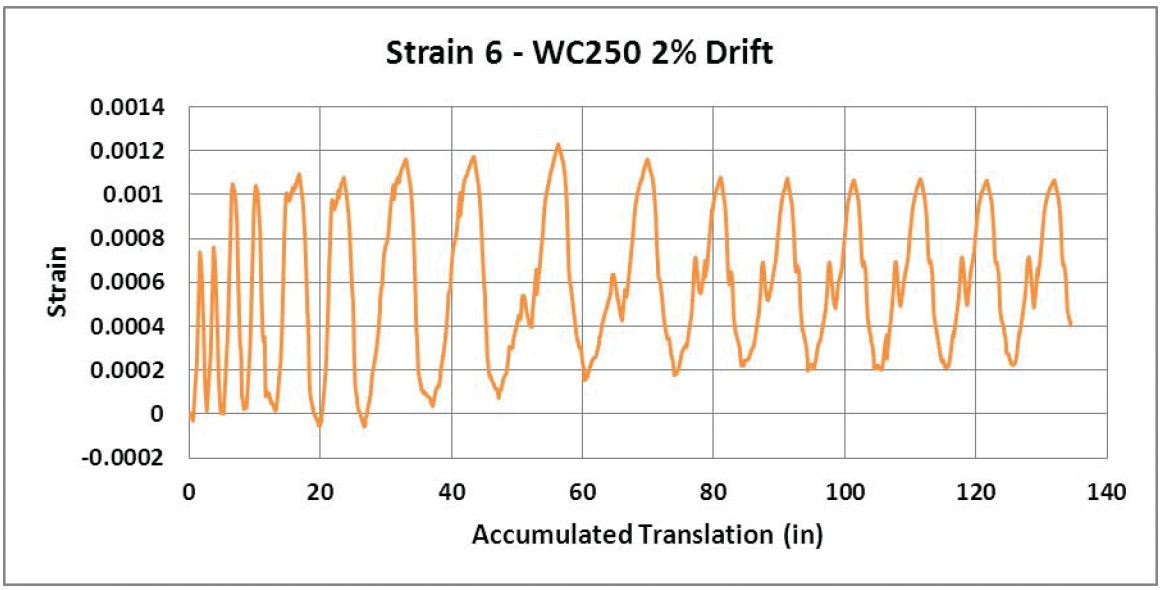

Fig. 19. Test 1, WC250 SG6.

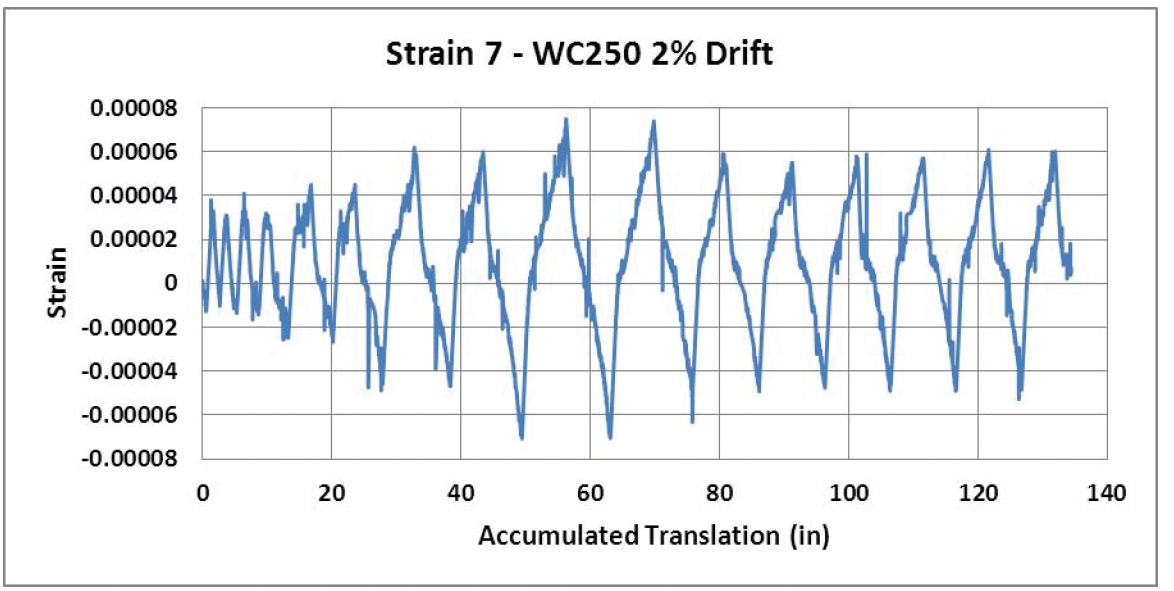

Fig. 20. Test 1, WC250 SG7.

SG1, SG2 and SG3 can be used to determine the state of strain (or stress) in the gusset plate along the brace located at the point of coincidence of the gages. (See Figure 9 and, for the WC 200, Figure 12.) Given the three normal strains at the peak load of 451 kips (2006 kN), the shear strain can be determined to be (229 μ, 6.6 ksi). This corresponds to the maximum principle shear stress of 25.0 ksi and principle normal stresses of 24.9 and 25.1 ksi. The von Mises yield criterion would predict yield at approximately $0.57 \times F_y = 20.8$ ksi. Therefore, the max shear stress in the gusset exceeded the theoretical yield stress at the maximum load during the test.

While the upper connection of the test specimen was not instrumented with strain gauges, visual inspection of the primary members and connection components after the test indicated no noticeable damage. In connecting the gusset plate to the web of the column, the relatively high out-of-plane flexibility of the column web appeared to accommodate frame rotation without distress to connection components or primary members. Primer paint on the column, except where removed to facilitate a Class A faying surface, showed no signs of distress at the connection to the column web. Consequently, in consideration of a repairable system, this configuration was demonstrated to be significantly more desirable than connecting to the column flange.

Test 2 Results: WC200 Brace

The WC200 test resulted in similar behavior to the WC250 test. Filtering similar to the previous test was used. Translation along the length of the brace was properly measured in this test and produced usable hysteretic information. The frame translation versus applied load also exhibited stable and repetitive behavior with positive incremental stiffness (see Figure 21).

The total brace elongation is illustrated in Figure 22. The second regimen of cycles for 3% drift begins at scan 6000. Translation along the brace shows a slightly asymmetric response to loading, with larger displacements in tension than in compression during the 2% test and larger displacements in compression than in tension during peak loads in the 3% test. The maximum elongation during the 2% drift test is 2.1 in. (53 mm) in tension and 1.9 in. (48 mm) in compression. The maximum elongation during the 3% drift test is 2.8 in. (71 mm) in tension and 2.9 in. (74 mm) in compression equal to 2.5 and 2.6% average strain, respectively.

Similar to the test of the WC250, visual inspection of the connection material after testing the WC200 suggested slip only occurred at connections that were designed assuming bolts in bearing. The brace-to-gusset connections that were designed slip-critical appeared to resist the load without slip as intended. Further, there was also no noticeable discontinuity between the brace translation and frame translation data, which also suggests slip did not occur at the brace-to-gusset connection where oversized holes were present.

Strain data for the WC200 test shown in Figures 23 through 28 display the two consecutive tests done with 2% drift first, followed by 3% drift. The second test at 3% drift begins at approximately scan 6000 (see Figure 22). The testing regimen reached an accumulated frame translation of 133.3 in. (3386 mm) during the 2% drift test and reached a total of 265.9 in. (6754 mm) by the end of the 3% test. The

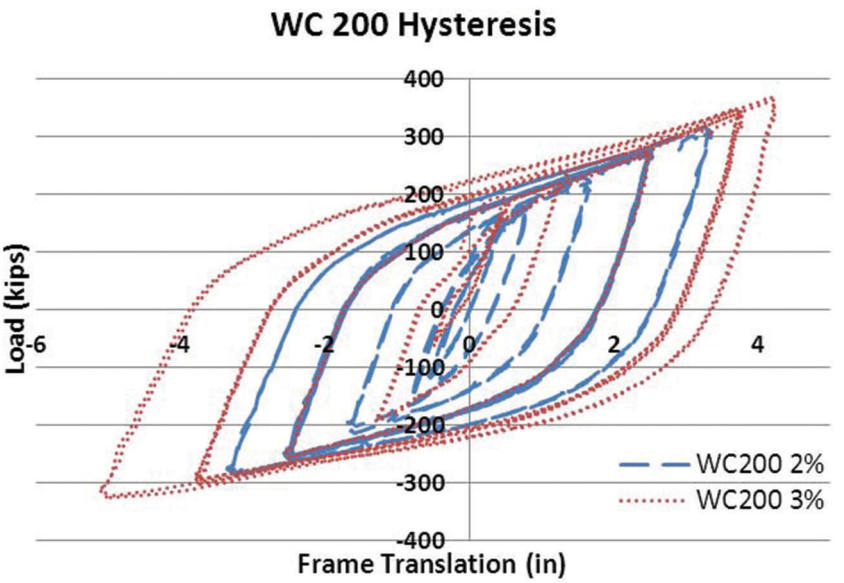

Fig. 21. Test 2, WC 200 load-translation.

cumulative inelastic axial brace deformation, as measured by the string pot on the exterior of the brace, was 64.1 in. (1628 mm) for the 2% drift test and 68.4 in. (1737 mm) for the 3% test. Thus, the total cumulative inelastic deformation was 132.5 in. (3366 mm), which corresponds to almost 800 times the calculated yield deformation or approximately four times the AISC minimum requirement.

SG7 at the top of the test frame was not measured in this test because of broken wiring. SG1 through SG5 showed behavior similar to that in the WC250 test. SG6 was at a different location in the WC200 test and measured the stresses in the beam web perpendicular to the long axis of the beam. It was observed by strain at SG4 that once the connection angle yielded, it performed at approximately the same strains during the 2% drift test as when subjected to 3% drift. The "upward ratcheting" of SG4 is due to yielding. Note that the downward shift is consistent with the yield strain of strain-hardened steel.

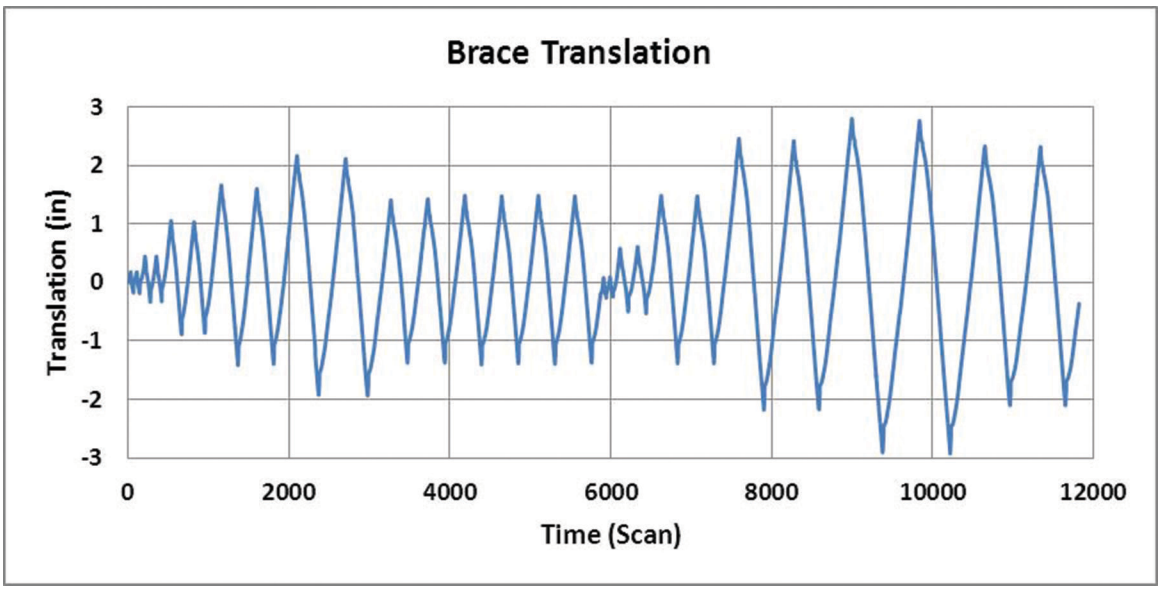

Fig. 22. WC200 brace translation.

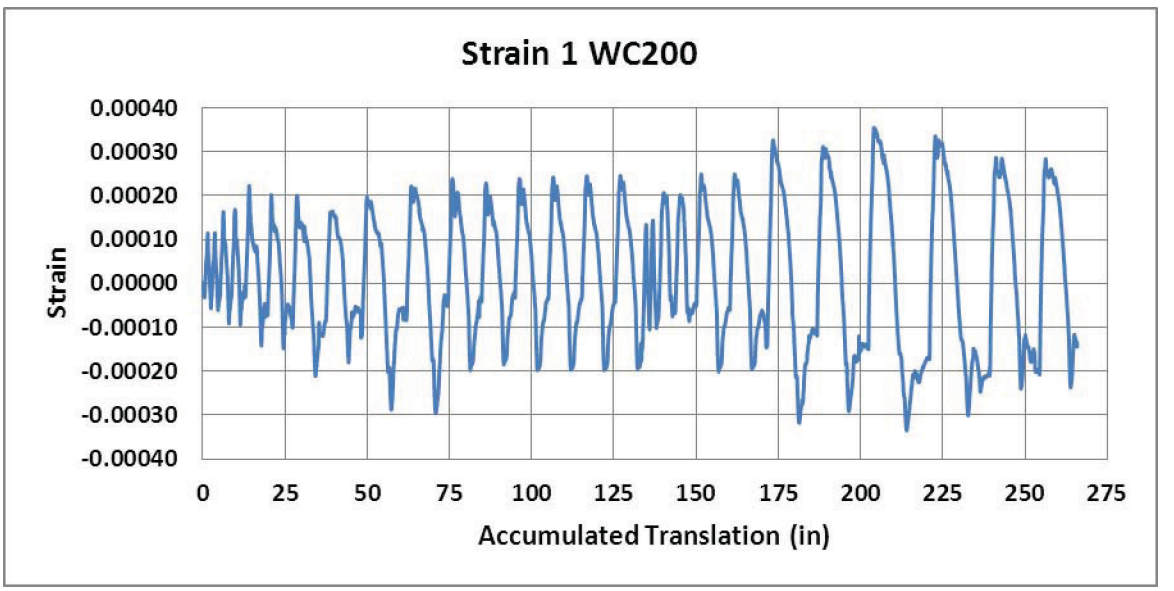

Fig. 23. Test 2, WC200 SG1.

SG5 and SG6 showed interesting behavior in the beam once they were subjected to the 3% drift cycles. It is observed that after an accumulated translation of 175 in. (4445 mm), SG5 shows the flange close to yield at a stress of 38.6 ksi (268 MPa); at the same time, SG6 shows that the web is yielding and reaching a strain of <6000 μ. At this cycle, the brace was in tension; however, because of the frame rotation, the angle between the column and beam closes and tends to "pinch" the gusset. This results in compression in the beam web. The web continued to exhibit some nonlinear behavior as it buckled slightly out of plane; thus, Figure 28 shows total strain (compression and bending) due to buckling.

Similar to the WC250, post-test visual inspection of the primary members and connection components at the upper connection indicated no noticeable damage. This again suggested that connecting one side of the gusset plate to a relatively flexible web of a primary member is desirable in consideration of a repairable system.

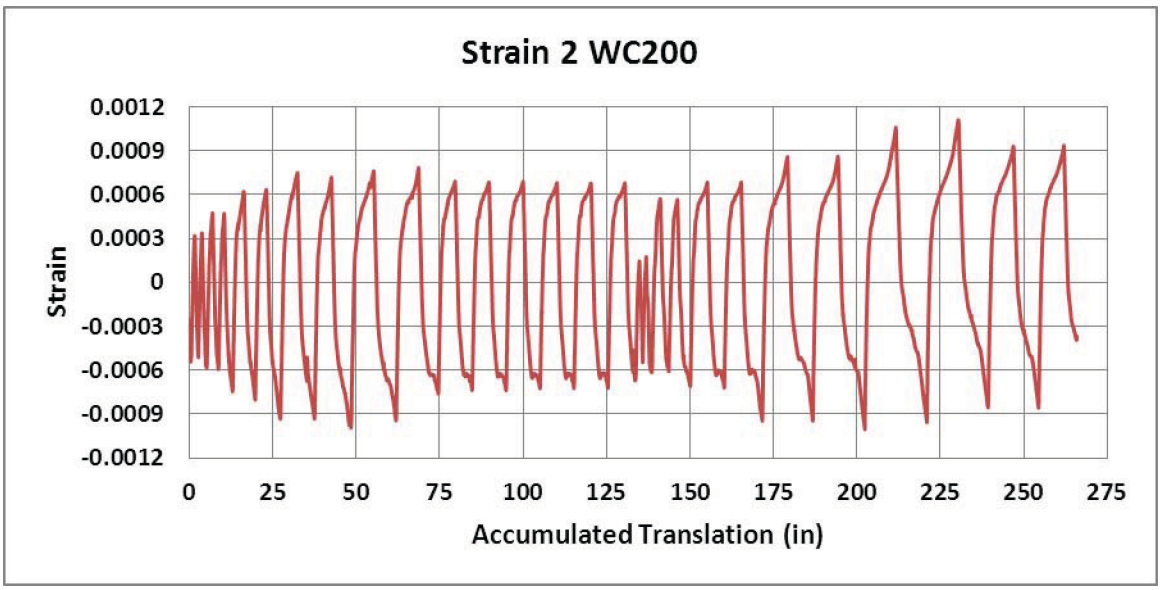

Fig. 24. Test 2, WC200 SG2.

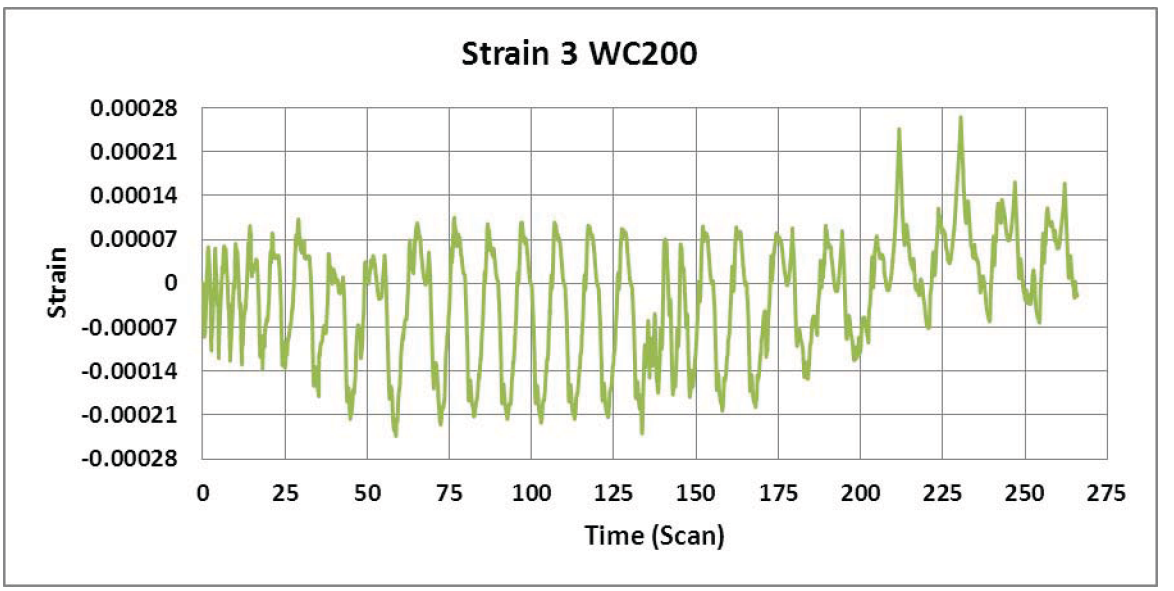

Fig. 25. Test 2, WC200 SG3.

NUMERICAL MODELING

The objective of analytical numerical modeling is twofold:

1. Use the available BRB design parameters to verify the design of the test frame and reaction frame.

2. Compare the numerical model to the observed test results with no "tuning" of the numerical model or BRB backbone curves.

Independent BRB Testing at University of Utah

With testing of the computer-simulated model, the linear and nonlinear behavior for the brace and test frame can be verified. Thus, methods for both linear and nonlinear frame analysis can be developed based on the test results. With this information, accomplishing the second objective provides valuable modeling parameters for use in designing and evaluating future frame and/or building models. Correct

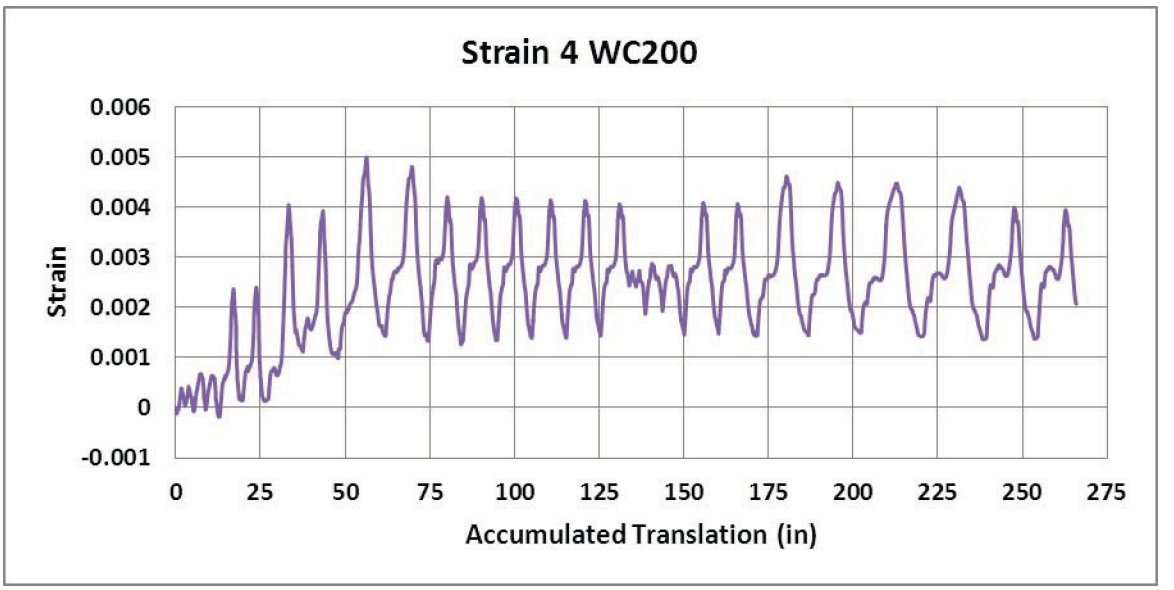

Fig. 26. Test 2, WC200 SG4.

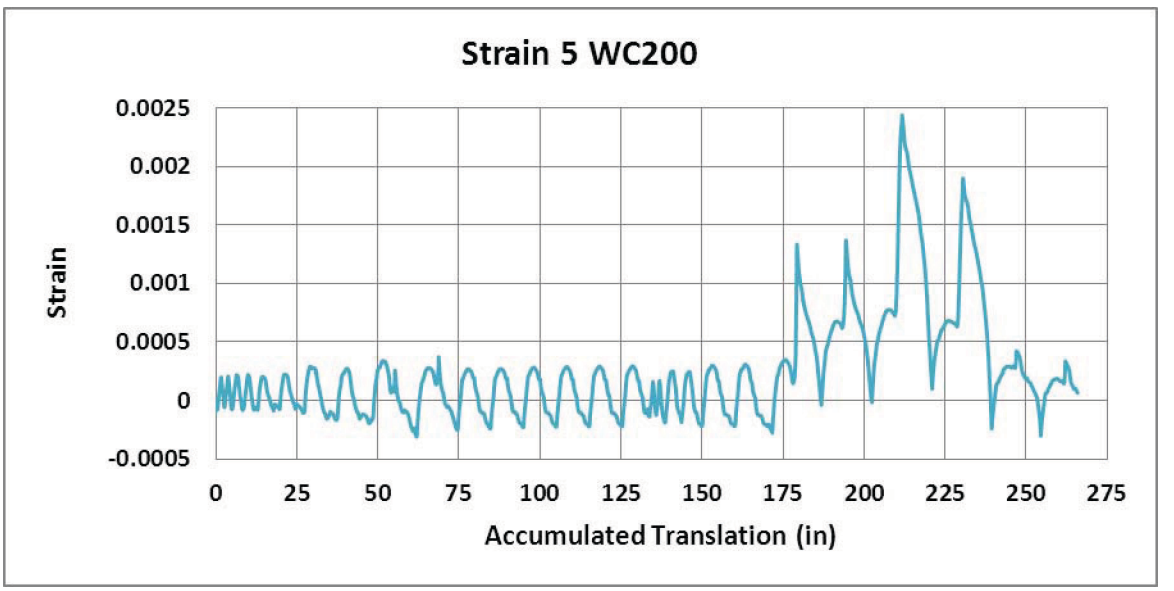

Fig. 27. Test 2, WC200 SG5.

stiffness, yield points, and BRB behavior can be determined for future use. Material and brace properties used are from previous research and testing performed outside of this project. Tensile strength for the brace cores were reported by MSI Testing and referenced by Star Seismic, which was also used in the numerical modeling [see McManus et al. (2011) for MSI results]. The tensile testing results are further discussed in the following section.

Research on the Star Seismic braces was referenced and reviewed prior to initial modeling of the braces and the test frame to verify the given Star Seismic parameters. Full-scale testing of the braces completed by Romero et al. (2007) provided regression equations to model the backbone curves that were normalized by yield strength. The results from axial tests performed on seven BRBs were compiled into a single plot to develop the tension and compression strain versus hardening curves (see Figure 29). Figure 30 illustrates typical results for a BRB, in this case a WC250. Note that a WC250 was used in one of the present tests.

The linear regression equations from the resulting curves were established; see Equations 1 and 2:

$$\omega = 26.90\varepsilon + 1.033 \quad (1)$$

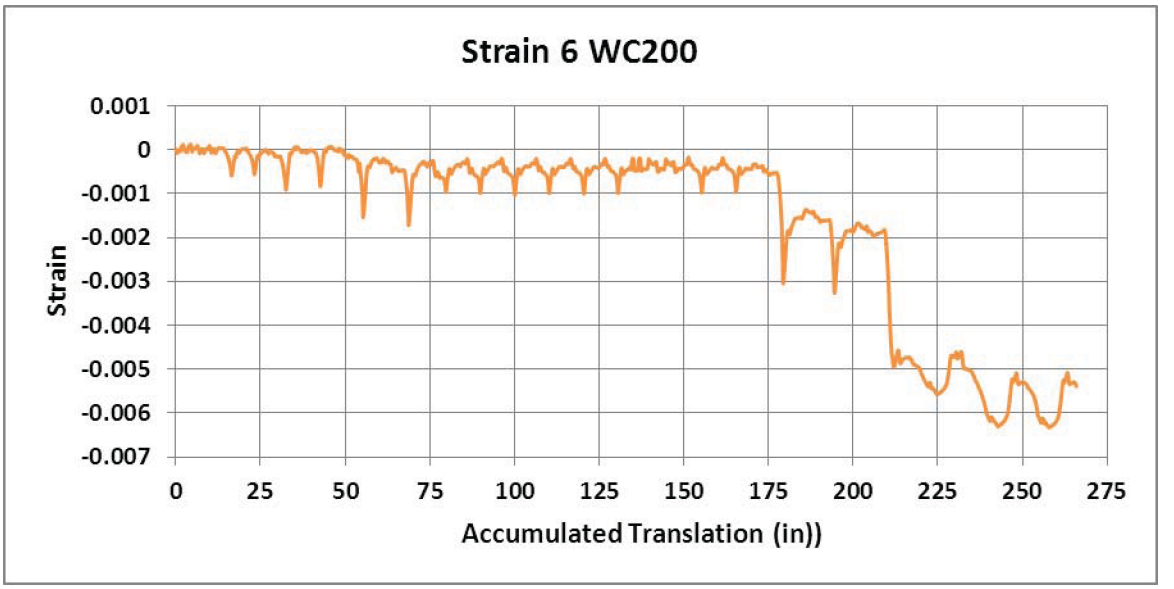

Fig. 28. Test 2, WC200 SG6.

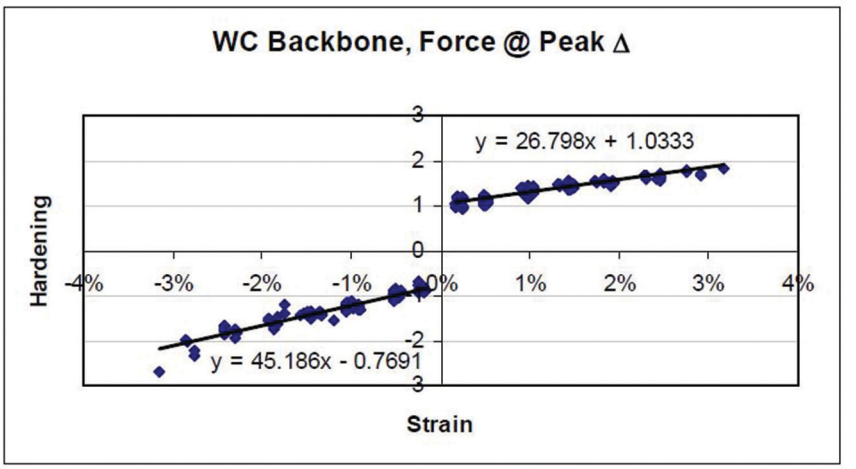

Fig. 29. WC backbone curve (Romero et al. 2007).

$$\omega\beta = 45.19\varepsilon - 0.77 \quad (2)$$

Equation 1 is the tension regression equation, and ω is the tension hardening (the load at maximum deformation normalized to yield stress). Equation 2 is the compression regression equation, and ωβ is the compression hardening.

The dashed line illustrated in Figure 30 approximates the backbone with a bi-linear function. The normalized version of this function is provided in Equations 1 and 2.

Star Seismic provided the University of Utah (Romero et al., 2007) a table with the dimension of the steel core for the braces, which was used to check the accuracy of a spreadsheet developed for the research herein, see Table 1.

For the WC200 and WC250 braces provided in this project, the dimensions were calculated from the shop drawings for input into the developed spreadsheet. See McManus et al. (2011) for the shop drawing.

Brace Modeling

In order to verify strength, results from tensile testing on the brace steel cores were provided by MSI Testing Inc. from Salt Lake City, Utah (test method ASTM 370). The report was referenced with the Nucor Mill Group of Jewett, Texas, report for the material properties of the core utilized in the Star Seismic braces. In the case of the steel used for the WC250, MSI Testing concluded that the average yield strength was 43.1 ksi (297.2 MPa), which was greater than that stated by the mill test report of 39.2 ksi (270.3 MPa). Star Seismic noted that the average from the MSI Testing report was used in the design of the braces; thus, the same value was used in this project. The same was not observed of the WC200 with an average test value of 43.2 ksi (297.9 MPa) and a mill reported yield strength of 43.5 ksi (300 MPa). Star Seismic used an average of the MSI Testing and the mill report for the WC200 with a value of 43.3 ksi (298.5 MPa).

The brace was first modeled based on the geometric information provided by Star Seismic, and using the brace backbone model (Romero et al., 2007), developed from the University of Utah's full-scale testing of WC series buckling restrained braces.

A backbone curve was developed from the University of Utah test data, based on the load at maximum deformation normalized to the yield load for each test specimen. Regression equations were developed to model the force versus translation relationship, including the elastic and inelastic behavior.

The areas and dimensions of the BRB steel-core extension plate, transition zone, core plate, and yielding zone were assumed to be proportional to the University of Utah (UT) test specimens. An individual stiffness value for the different zones within the steel core was calculated based on area multiplied by the modulus of elasticity divided by the length. The effective stiffness was then calculated by assuming the individual sections would act as springs in series as

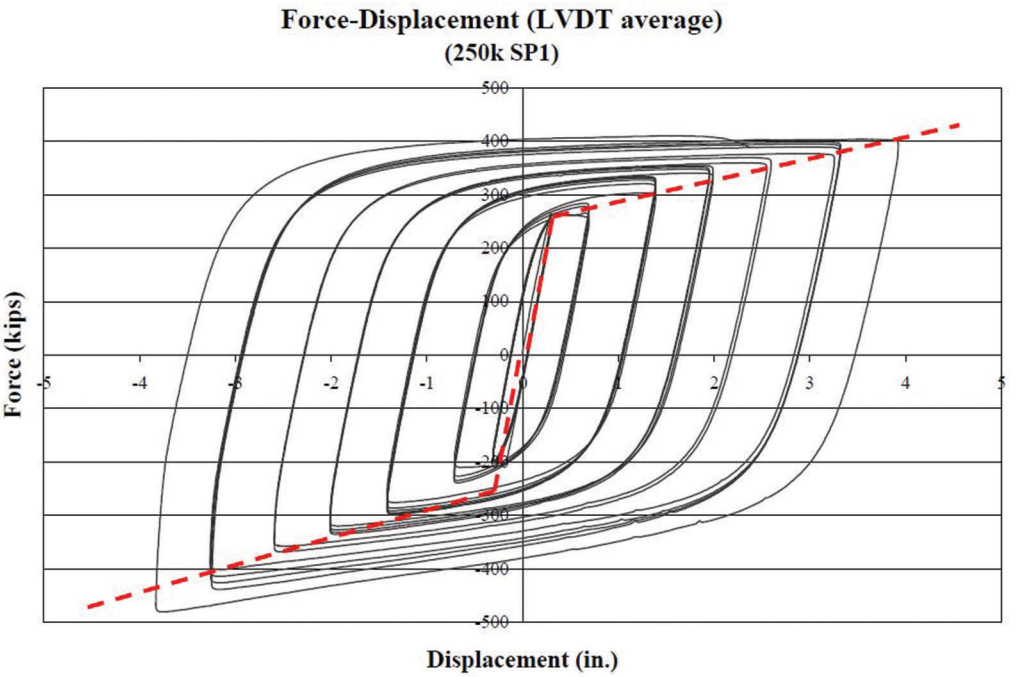

Fig. 30. Typical load translation test result (WC250) (Romero et al., 2007).

Table 1. Dimensions of Steel Core for the Braces (Romero et al., 2007)						
			Brace Designation			
			WC150	WC250	WC500	WC780
Specified Yield Strength, F_y, ksi			41.4	39.9	39.9	39.9
Extension Plate (*KP*)		Thickness, t_{KP}, in.	0.75	2	2	4
		Width, b_{KP}, in.	9	9	9	18.5
		Length, L_{KP}, in.	13	19	23	23
		Stiffness, K_{KP}, kip/in.	15,058	27,474	22,696	93,304
Core Plate	Number of Plates		1	1	2	4
		Thickness, t_p, in.	0.75	1	1	1
		Total Thickness, t_T, in.	0.75	1	2	4
	Transition Zone (*TZ*)	Width, b_{TZ}, in.	10	10	10	10
		Length, L_{TZ}, in.	14	14	14	14
		Stiffness, K_{TZ}, kip/in.	15,536	20,714	41,429	82,857
	Yielding Zone (*YZ*)	Width, b_{YZ}, in.	4.90	5.75	5.75	4.88
		Length, L_{YZ}, in.	152.7	134.7	134.7	132.6
		Stiffness, K_{YZ}, kip/in.	698	1,238	2,476	4,269

illustrated in Figure 31. The springs represent the transition, core, and extension plates. The equivalent elastic stiffness is computed from:

$$K_{equivalent} = \left[\frac{1}{k_1} + \frac{1}{k_2} + \frac{1}{k_3}\right]^{-1}$$

Given the shop drawings and information, the effective stiffness for the WC200 and WC250 was determined using the assumptions previously stated. The calculated effective stiffness values were used in SAP2000 v12, hereafter referred to as SAP2000, with multilinear links to model the response of each BRB. A multilinear link and a Wen model were created to ensure that the multilinear response was accurate when compared with the UT data for validation (SAP2000 v12).

Again, the inelastic behavior was modeled using the UT backbone curves. Figures 32 and 33 illustrate the SAP2000 models of a single BRB using the multilinear plastic model, the Wen model and data from one of the University of Utah WC250 tests.

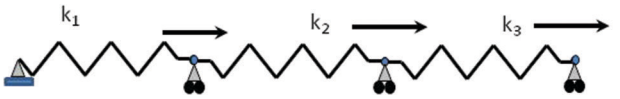

Fig. 31. Springs in series.

By comparison, the SAP2000 modeling of single BRBs is more of a coarse approximation of the actual behavior as demonstrated by the University of Utah testing results. Also, it is shown that the numerical model does not develop any asymmetrical pattern as does the actual brace when loading compression versus tension. Additionally, the SAP2000 model is based upon a kinematic strain-hardening model, while the exhibited behavior is more isotropic. Although the backbone curve is modeled reasonably well, the total energy absorbed within the model is not as large as the exhibited behavior because part of the hysteric area is missing. The model would be adequate in developing a push-over curve, but would perhaps be overly conservative in modeling a time-history event.

Full-Frame Modeling

Due to the complexity of modeling the entire testing apparatus in SAP2000, the frame was modeled in multiple steps. First, the geometry of the frame was modeled with undefined shapes and stiffness to determine which frame members would be necessary for the full analytical model (see Figure 34). Based on a nominal 100-kip (445-kN) load applied to the top of the frame, each member was analyzed for axial and shear forces to determine its influence on the system during testing. Initial modeling of the angles bracing the test specimen from movement out-of-plane of the load direction were removed due to an undesirable transfer of shear forces to the test frame in the SAP2000 model. These angles were connected with single-bolt pinned ends in the actual test assemblage and did not resist any shear forces as they

slipped and rotated under frame translations. Constraints were imposed on the nodes where the angles connected to the test specimen as a more effective means of modeling the system. When modeling the large rigid plate connecting the test reaction frames to the test frame, it was determined that deformations in the plate were small enough that the connection could be assumed rigid, the expected result.

More load-tracking review was done in SAP2000. By observation, and as expected, it was determined that the majority of the deformation was occurring in the test specimen due to the much greater stiffness of the reaction frames (see Figure 35).

The next step was to model the test frame alone with constraints on the nodes that would normally be attached to the reaction frame. A few assumptions were made to simplify the model. Connections were assumed to be either rigid or fully pinned because the actual stiffness of the connections was not fully known. The previously developed links were

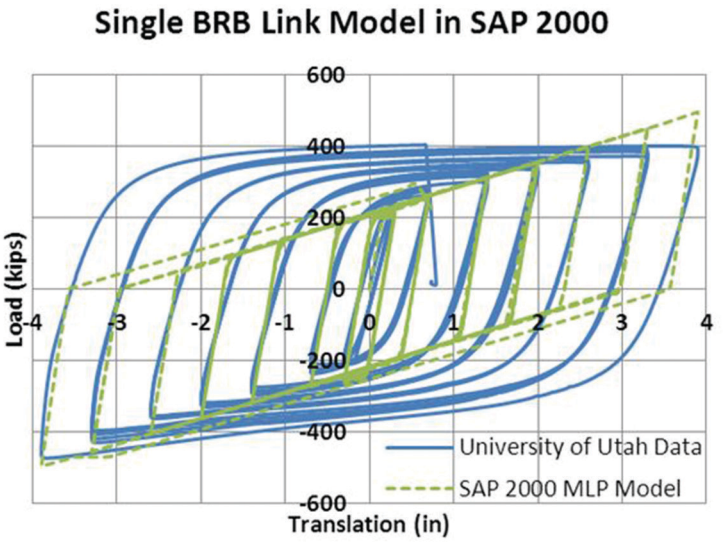

Fig. 32. Single BRB link multilinear plastic model vs. University of Utah test data.

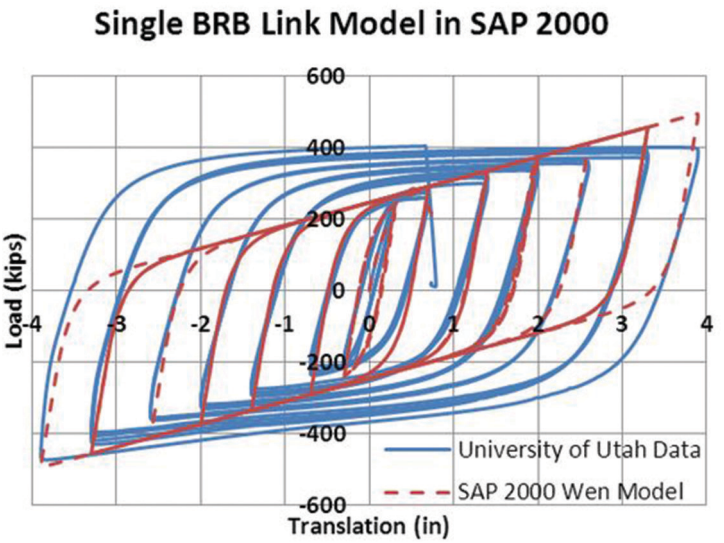

Fig. 33. Single BRB link Wen model vs. University of Utah test data.

imported into the test specimen model and placed appropriately (see Figure 36). With the 100-kip (445-kN) load applied to the test specimen, it was determined that the link was working properly when compared with hand computations.

COMPARISON OF NUMERICAL MODELING AND EXPERIMENTAL RESULTS

By using the link developed in SAP2000, it was possible to run the same time-history test on the analytical model as was done on the physical test frame. The target translations for the experimental testing were input into SAP2000, and a displacement controlled loading cycle was run. The results from the multilinear model of the brace were then plotted against the experimental data for comparison (see Figures 37 and 38). In order to produce a more accurate comparison, the output from the SAP2000 model was link force, column shear and axial force in the top beam, which is equivalent to the pressure gauges in the actuator measuring

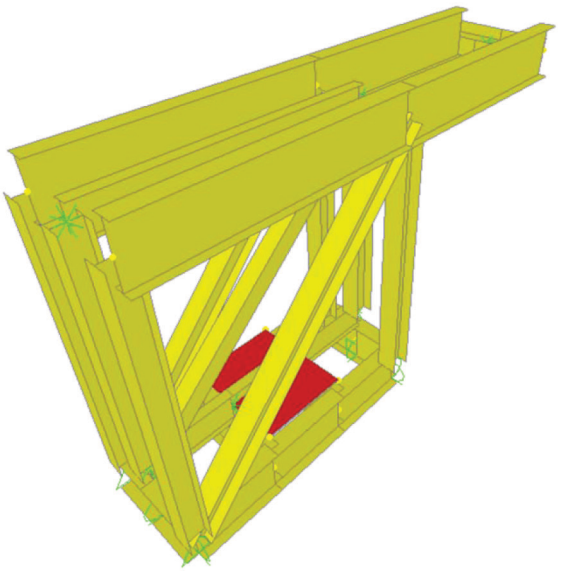

Fig. 34. Initial full frame model in SAP2000.

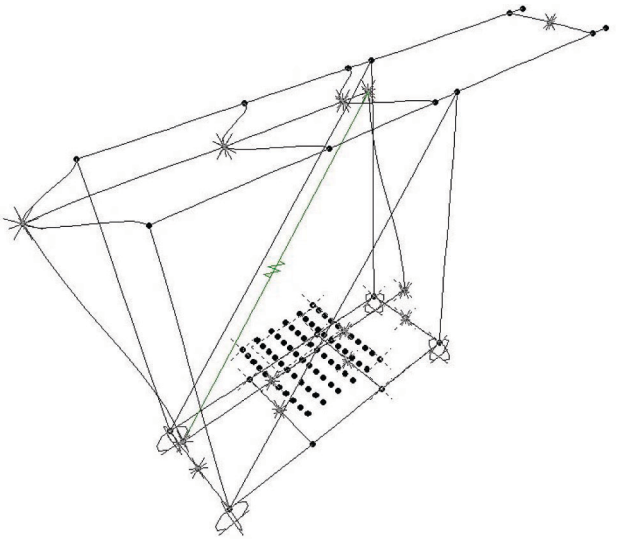

Fig. 35. Full-frame deformed shape with 100-kip load (SAP2000).

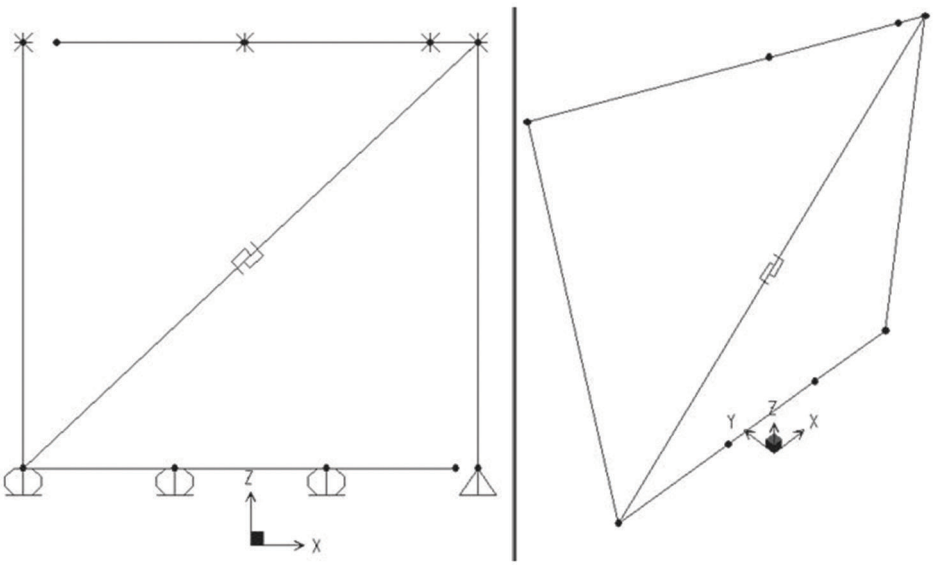

Fig. 36. Simplified analytical model (SAP2000).

forces on all these elements during the test. Notably, the multilinear model behaved similarly to the experimental model. The WC200 model did predict a slightly higher peak load at maximum positive translation, but at the maximum negative translation, the model and experimental data are almost identical. The WC250 model is much more in line with the experimental data and is even slightly conservative at maximum negative translation, having a peak load slightly lower than the experimental data.

Utilizing Wen modeling of the two braces produced a more accurate hysteresis of the frame behavior than the multilinear plastic models. The hysteretic loops match more closely with the test data, as shown in Figures 39 and 40, and had a slightly higher value at the maximum displacement, similar to the multilinear plastic model. These similarities suggest that the backbone curve developed from the University of Utah test gives proper values for modeling.

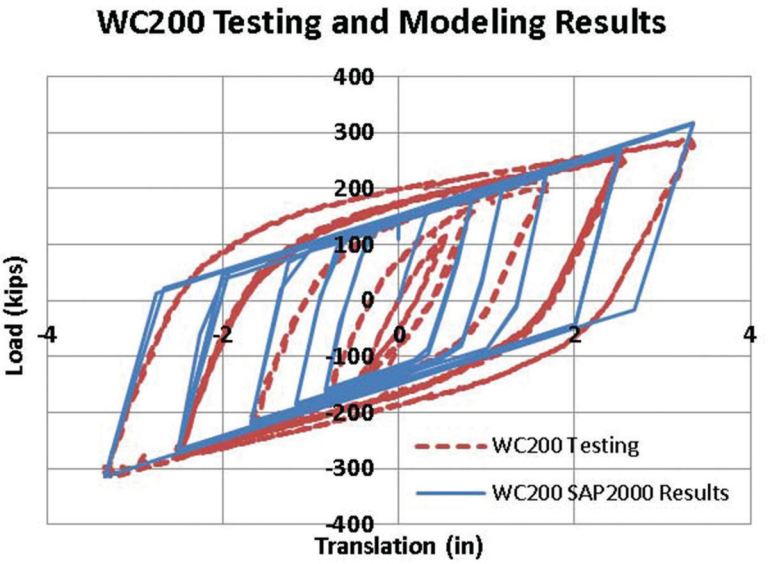

Fig. 37. WC200 testing and multilinear plastic modeling results.

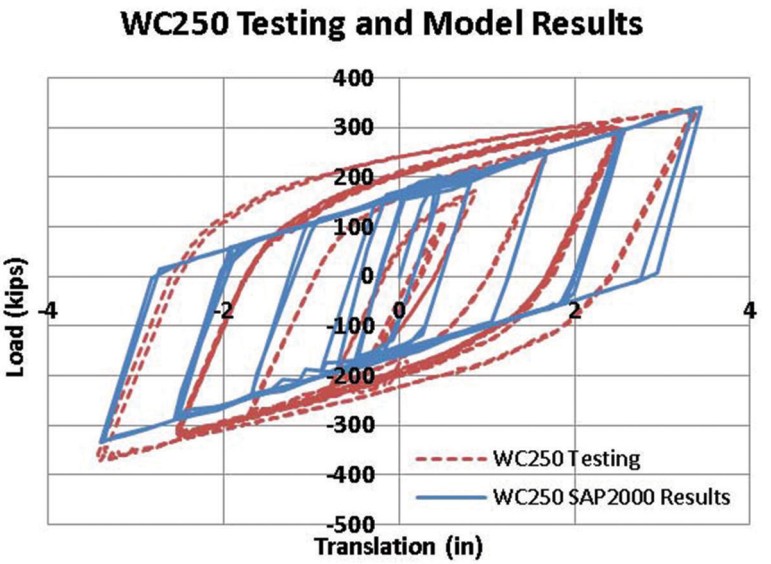

Fig. 38. WC250 testing and multilinear plastic modeling results.

It should be noted that both the multilinear and the Wen models are fully symmetrical in their response to loads in tension and compression. This explains the minor offset when comparing the testing results to the SAP2000 modeling because the BRB does perform somewhat different in tension versus compression.

DESIGN RECOMMENDATIONS

The research herein has shown that with proper compression strength and strain-hardening adjustment factors for the buckling restrained brace, the connection design provisions of the AISC *Specification* and AISC *Seismic Provisions* result in desirable braced frame behavior using fully

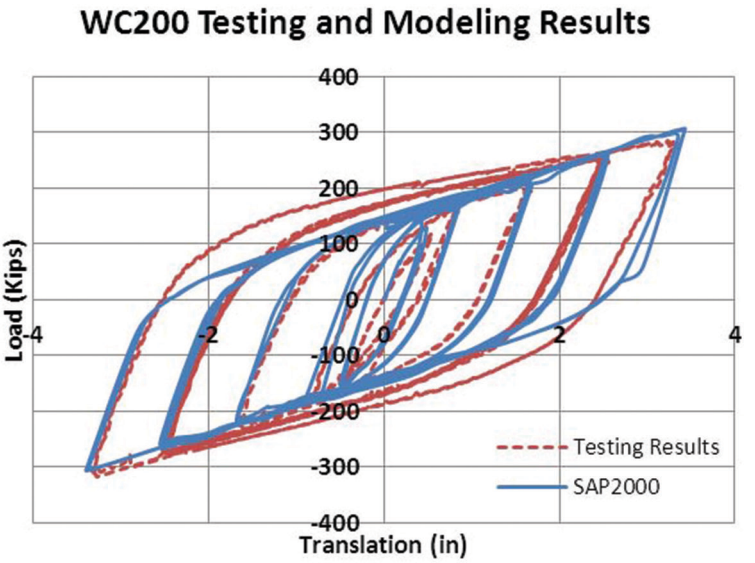

Fig. 39. WC200 testing and Wen modeling results.

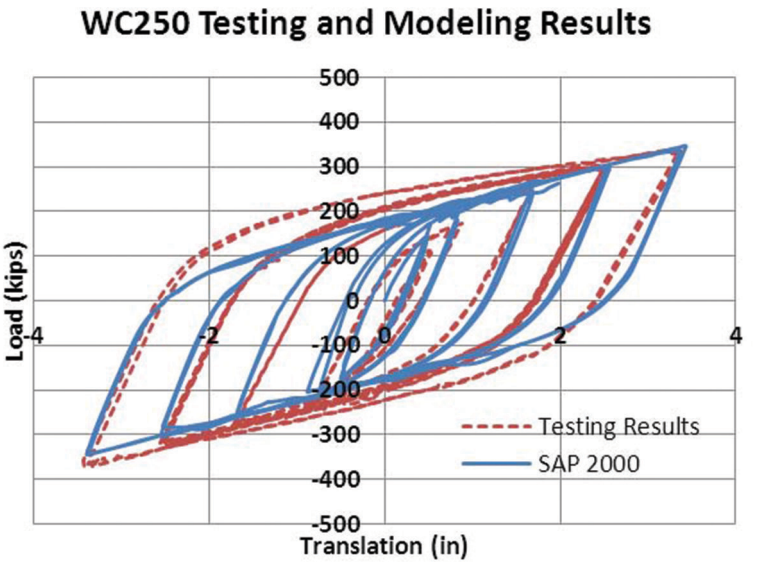

Fig. 40. WC250 testing and Wen modeling results.

bolted connections. In addition to the provisions of these documents, the following general recommendations are made to facilitate constructability and maximize connection strength. Furthermore, the following serviceability recommendations are made to promote an easily repairable system in which inelastic damage to the primary beams and columns are minimized.

General Recommendations

1. Bearing bolts in standard holes or slip-critical bolts with oversized holes in one ply of connecting interfaces may be used to connect the ends of buckling restrained braces to gusset plates.

2. Bearing bolts in standard holes should be used to connect gusset plates to double-angle connection assemblies and double-angle connection assemblies to primary beams and columns.

3. Bolt rows in the connection-angle assemblies may be aligned or staggered. Staggered assemblies are recommended to allow for reduced bolt gauges on the flanges of the primary members.

Repairable Recommendations

1. Beam and column flange thickness should exceed connection-angle thickness to limit bolt-bearing deformations in the primary members.

2. To reduce the possibility of inducing yield in the beam or column flange, the bending capacity of the primary member flange—including the effects of prying action—should exceed that of the outstanding legs of the connection angles. Primary members should be oriented such that at least one side of the gusset plate is connected to the web of either the beam or the column.

   Orienting primary members such that the gusset plate is connected to the flange of both the beam and the column results in "pinching" forces between the gusset plate and primary members, which can result in local damage to the primary members. These forces are alleviated by connecting one side of the gusset plate to the web of a primary member because of the relative out-of-plane flexibility of the member web.

CONCLUSIONS

The following conclusions are drawn from the experimental testing and numerical modeling of both the full frame and the individual braces.

1. In reference to AISC *Seismic Provisions* acceptance criteria, testing of the full-scale, fully bolted buckling restrained braced frame met all strength requirements and exceeded the required testing regimen of 2% drift associated with an assumed 1% design story drift.

2. Provisions of the AISC *Specification* and AISC *Seismic Provisions* are appropriate for fully bolted BRBF connections. The use of the uniform force method and the uniform force method—special case 2, minimizing Shear in the Beam-to-Column Connection," was shown to be appropriate for connection force distribution.

3. The frame design exhibits the ability to withstand multiple seismic events without fracture, brace or primary framing member instability or without brace-end connection failure.

4. The ability to easily replace the braces and connection components was demonstrated. Thus, the reparable advantage of the all-bolted connections was revealed.

5. Orienting columns such that the gusset plate is connected to the column web allows for rotation of the gusset connection under large drifts without noticeable damage to the primary beams and columns.

6. Orienting columns such that the gusset plate is connected to the column flange results in connection restraint against frame rotations that can cause damage to unstiffened primary beams and columns.

7. The methods used to develop a numerical model of the buckling restrained braces in SAP2000 were effective and could be easily adapted to different brace sizes for various systems. Utilization of the link properties in a full-frame model accurately predicted behavior of the system. Multilinear approximation was adequate to model the behavior of the BRB in the frame, but the Wen model provides a more accurate prediction including the nonlinear transition near yield.

ACKNOWLEDGMENTS

The authors would like to recognize Puma Steel, AISC, Nucor Fastener and the University of Wyoming for funding, fabrication and material donations, without which this project would not have been possible.

REFERENCES

AISC (2005a), *Seismic Provisions for Structural Steel Buildings*, American Institute of Steel Construction, Chicago, IL.

AISC (2005b), *Specification for Structural Steel Buildings,* American Institute of Steel Construction, Chicago, IL.

AISC (2005c), *Steel Construction Manual*, 13th ed., American Institute of Steel Construction, Chicago, IL.

ASCE (2007), "Seismic Rehabilitation of Existing Buildings," ASCE Standard ASCE/SEI 41-06, American Society of Civil Engineers, Reston, VA.

FEMA (2003), "Recommended Provisions for Seismic Regulations for New Buildings and Other Structures,". FEMA-450, Part 2: Commentary, Federal Emergency Management Association, Washington, DC.

FEMA (2008), "HAZUS® MH Estimated Annualized Earthquake Losses for the United States," FEMA-366, Federal Emergency Management Association, Washington, DC.

IBC (2006), *2006 International Building Code,* International Code Council.

IBC (2009), *2009 International Building Code,* International Code Council.

Lopez, W.A., Gwie, D. S., Lauck, T.W. and Saunders, C.M. (2004), "Structural Design and Experimental Verification of a Buckling-Restrained Braced Frame System," *Engineering Journal*, AISC, Fourth Quarter, pp. 177–186.

McManus, P.M. and Puckett, J.A. (2011), "Repairable Seismic Moment Frames with Bolted WT Connections: Part I," *Engineering Journal*, AISC, Fourth Quarter, pp. 265–281.

McManus, P.M., Puckett, J.A. and MacMahon, A. (2011), "Economic and Serviceable Seismic Systems, Phase II—All-Bolted Buckling Restrained Braced Frames," AISC Report, Department of Civil and Architectural Engineering, University of Wyoming, Laramie, WY.

Romero, P., Reaveley, L., Miller, P.J. and Okahashi, T. (2007), "Full Scale Testing of WC Series Buckling-Restrained Braces," Department of Civil and Environmental Engineering, University of Utah, Salt Lake City, UT.

Thornton, W.A. and Muir, L.S. (2009), "Design of Vertical Bracing Connections for High-Seismic Drift," *Modern Steel Construction*, AISC, March, pp. 61–64.